Adsorption of 3-Thiophene Carboxylic Acid on Silver Nanocolloids: FTIR, Raman, and SERS Study Aided by Density Functional Theory

ARTICLE *in* THE JOURNAL OF PHYSICAL CHEMISTRY C · JULY 2011

Impact Factor: 4.77 · DOI: 10.1021/jp204297y

4 AUTHORS, INCLUDING:

Subhendu Chandra
Victoria Institution (College)
5 PUBLICATIONS **39** CITATIONS
SEE PROFILE

Joydeep Chowdhury
Jadavpur University
71 PUBLICATIONS **631** CITATIONS
SEE PROFILE

Manash Ghosh
Indian Association for the Cultivation of Scie…
57 PUBLICATIONS **621** CITATIONS
SEE PROFILE

THE JOURNAL OF PHYSICAL CHEMISTRY C

ARTICLE

pubs.acs.org/JPCC

Adsorption of 3-Thiophene Carboxylic Acid on Silver Nanocolloids: FTIR, Raman, and SERS Study Aided by Density Functional Theory

Subhendu Chandra,[†,∥] Joydeep Chowdhury,[*,‡,#] Manash Ghosh,[§,⊥] and G. B. Talapatra[*,§,⊥]

[†]Department of Physics, Victoria Institution (College), 78 B, A. P. C. Road, Kolkata-700009, India

[‡]Department of Physics, Sammilani Mahavidyalaya, Baghajatin Station, E.M. Bypass, Kolkata-700075, India

[§]Department of Spectroscopy, Indian Association for the Cultivation of Science, Jadavpur, Kolkata-700 032, India

ABSTRACT: The concentration and pH dependent surface-enhanced Raman scattering (SERS) study of the industrially and biologically significant 3-thiophene carboxylic acid (3-TCA) molecule has been investigated. The SERS spectra of the molecule at different C_{Ad} values are compared with its FTIR spectrum and normal Raman spectra (NRS) in varied environments. The optimized structural parameters and computed vibrational wavenumbers of the neutral and the anionic (3-TCA$^-$) forms of the molecule have been estimated from density functional theory (DFT) calculations. The vibrational signatures of the molecule have been assigned from the potential energy distributions (PEDs). The concomitance of the Raman bands representing vibrational signatures emanating from the neutral and the anionic forms of the molecule signify the presence of both the forms of the molecule in the solid state and in acetonitrile (ACN) solution. However, detailed vibrational analysis reveals that 54% of 3-TCA is prevalent in the solid state while 63% of 3-TCA$^-$ is predominate in ACN solution at neutral pH. Concentration dependent SERS spectra reveal that the anionic form of the molecule is adsorbed on the nanocolloidal silver surface with the molecular plane tilted or nearly flat with respect to the surface. The genesis of selective enhancements of the Raman bands in the SERS spectra of the molecule has been unveiled from the view of Albretcht's *A* contribution and Herzberg—Teller's charge transfer contribution.

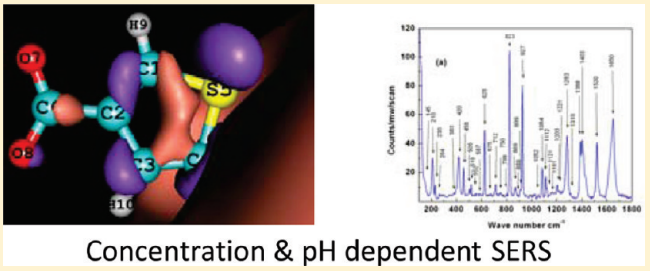

1. INTRODUCTION

Surface enhanced Raman scattering (SERS) is a well-established and highly effective technique of observing Raman scattering from species present at trace concentrations down to the single molecule detection level.[1] It is a useful tool in surface chemistry because of its high sensitivity and potential in providing useful information regarding metal—adsorbate interactions.[2,3] The adsorptive site/sites and the orientation of the adsorbed molecule can be determined qualitatively by comparing the relative intensities and positions of the bands in the SERS with those in the Raman spectrum of the pure or solvated analyte.[3,4] Despite intensive theoretical works[5] and publications of excellent reviews,[6] the exact nature of the huge enhancement in Raman cross sections found in SERS is still a matter of debate. However, it is generally accepted that two enhancement mechanisms, one a long-range electromagnetic (EM) effect and the other a short-range chemical (CHEM) effect, are simultaneously operative. The EM mechanism is based on the amplified electromagnetic field generated upon optical excitation of surface plasmon resonance of nanoscale surface roughness.[7] The CHEM mechanism, also referred to as the charge transfer (CT) mechanism, involves the photoinduced transfer of an electron from the Fermi level of the metal to an unoccupied molecular orbital of the adsorbate or vice versa depending on the energy of the photon and the electric potential of the interface.[8] Recently, quantum chemical calculations and molecular dynamics simulation studies are successfully utilized to model the experimentally observed SERS spectra.[9]

Among the family of the five-member heterocycles, thiophene and its derivatives have basic importance in chemistry.[10] Thiophenes, also known as thiofurans, are the simplest representatives of stable aromatic structures bearing a sulfur atom and share some similar chemical properties with benzene. The sulfur atom in the five-member ring acts as an electron donating heteroatom by contributing two electrons to the aromatic sextet, and thiophene is thus considered to be an electron-rich heterocycle. Thiophene and its derivatives exist in petroleum or coal, and they are found in natural plant pigments. A water-soluble B-complex vitamin, biotin, is a reduced thiophene derivative. Thiophene derivatives are extensively used in the manufacturing of dyes, aroma compounds, and pharmaceuticals. The large number of reports pertaining to the synthesis of thiophene and its derivatives indicate the continuing importance of these compounds in biology,[11] chemistry,[12] industry,[13] and medicine.[14] These derivatives are reported to act as inhibitors of bone resorption in tissue culture.[15] They are used as monomers to make condensation copolymers. π-Conjugated polythiophenes and their derivatives have attracted considerable interest among fundamental and applied researchers because of their one-dimensional intrinsic properties and potential uses for commercial applications in the field of molecular electronics.[16]

Received: May 9, 2011
Revised: June 16, 2011
Published: June 21, 2011

Considering the enormous industrial and biological importance, the present work has been undertaken with the primary aim of studying the preferential existence of the neutral and/or anionic forms of 3-thiophene carboxylic acid (3-TCA) in solid and in acetonitrile (polar) solvent. Experimental support for the existence of the preferential forms of the molecule was gained from the normal Raman spectra (NRS) and Fourier transform infrared (FTIR) spectra. To the best of our knowledge, no vibrational analysis of the molecule has been reported, though its thermophysical and thermochemical properties as a function of temperature have been published in the literature.[16] This manuscript may be considered as the first report of the vibrational assignment of the molecule. Further insight into the molecular structures and the theoretical estimation of the vibrational signatures of the neutral and the anionic forms of the molecule are provided from the theoretical calculations using density functional theory (DFT). The adsorptive behavior of the preferential form of the molecule on the nanocolloidal silver surface at various pH values and also at different adsorbate concentrations (C_{Ad}), close to that encountered under physiological conditions in living systems, has been elucidated from the SERS spectra. The genesis of selective enhancements of the Raman bands in the SERS spectra of the molecule has been unveiled from the view of the Albrecht's *A* contribution and the Herzberg−Teller (HT) CT contribution.

2. EXPERIMENTAL SECTION

The 3-TCA molecule was purchased from Aldrich Chemical Co. and used after repetitive crystallization. The molecule is insoluble in water but readily soluble in acetonitrile (ACN). Silver nanocolloids were prepared by the process of Creighton et al.[17] The stable yellowish sol thus prepared shows a single extinction maximum at 392 nm, and it was aged for 2 weeks before being used in the experiment. The size of the silver particles in this sol is known to be in the range 1−50 nm.[18] All the required solutions were prepared with distilled and deionized water from a Milli-Q apparatus (Millipore, USA) via an ELIX system. Mixing a specific volume of stock solution with an appropriate volume of silver nanocolloid attained the desired concentration of the probe molecule in the silver colloid.

2.1. Instrumentation. Raman spectra were recorded with a Spex double monochromator (model 1403) fitted with a holographic grating of 1800 grooves/mm and a cooled photomultiplier tube (model R928/115) from Hamamatsu Photonics, Japan. The sample was taken in a quartz cell and was excited with 514.5 nm radiation from a Spectra Physics Ar^+ ion laser (model 2020-05) at a power of 200 mW. Raman scattering was collected at a right angle to the excitation. The operation of the photon counter, data acquisition, and analyses were controlled with Spex Datamate 1B. The acquisition time by the spectral element was 0.5 s. The scattered light was focused onto the entrance slit of width ∼4 cm^{-1}. Polarized Raman spectra were recorded with an arrangement provided with the instrument. The accuracy in the measurement was ±1 cm^{-1} for strong and sharp bands and slightly less for other bands. The FTIR spectra of the powder samples were taken in a KBr pellet using a Nicolet Magna-IR 750 spectrometer series II. The resolution of the infrared band was about 4 cm^{-1} for sharp bands and slightly less for broader bands. The absorption spectra were recorded on a Shimadzu 2010 PC UV−vis spectrophotometer. All the spectra reported in the figures are original raw data directly transferred from the instrument and processed using the Microcal origin version 8.0.

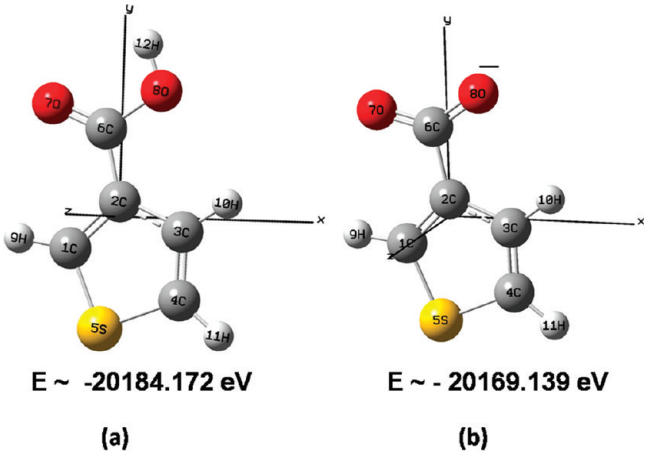

Figure 1. Optimized molecular structure of the (a) neutral and (b) anionic forms of the molecule obtained from the B3LYP/aug-cc-PVTZ level of theory.

3. COMPUTATIONAL DETAILS

The theoretical calculations were carried out using Gaussian 03 operated in the Linux system.[19] Optimization of the molecular structures and the calculations of the vibrational frequencies were done by density functional theory (DFT). The B3LYP functional[20] and aug-cc-PVTZ[21] basis set with the keyword IOp (7/33 = 1, 7/32 = 1) in the route section were used in the DFT calculations. The keyword IOp (7/33 = 1, 7/32 = 1) enables one to obtain the Cartesian "L" matrix in the output file. The theoretically estimated vibrational frequencies of both the neutral and the anionic forms of the molecule were scaled by the scaling factor 0.995. The potential energy distribution (PED) was performed with GAR2PED[22] in terms of internal coordinates of the molecule from the output of the DFT calculations. Cartesian displacements and calculated vibrational modes of the molecules have been displayed using Gauss View-03 software. Information pertaining to the excited states of the anionic form of the molecule was obtained by calculating the Franck−Condon (FC) transition energies for the B3LYP/aug-cc-PVTZ optimized ground state structures at the configuration interaction single (CIS)/aug-cc-PVTZ level of theory. In the process of geometry optimization for the fully relaxed method, convergence of all the calculations and the absence of imaginary values in the wavenumbers confirmed the attainment of local minima on the potential energy surface. 2D-correlation spectroscopic studies were performed using 2D Shige version 1.3 software.[23] Prior to 2D analysis, five-point smoothing for all the SERS bands of the molecules was carried out after baseline correction in order to remove the spectral artifacts. The pK_a value and the isoelectric point (PI) of the molecule were estimated theoretically using the Marvin 5.1.0 software.[24]

4. RESULTS AND DISCUSSION

4.1. Molecular Structure. The 3-TCA molecule can exist in neutral and in anionic (3-TCA^-) forms. The calculated molecular structures of 3-TCA and 3-TCA^- are shown in panels a and b of Figure 1, respectively. In order to retrieve some ideas about the relative stabilities of different forms of the molecule in the gas phase, the minimum energies of the molecule at its respective optimized geometries have been computed using the DFT method. The theoretical results indicate that the SCF energy

Table 1. Relevant Structural Parameters of the 3-TCA and 3-TCA$^-$ Forms of the Molecule Calculated from the B 3LYP/aug-cc-PVTZ Level of Theory

	3-TCA	3-TCA$^-$
	Bond Length (Å)	
C_1-C_2	1.37	1.36
C_1-S_5	1.71	1.73
C_3-H_{10}	1.08	1.08
C_4-S_5	1.73	1.74
C_6-O_8	1.36	1.25
C_4-H_{11}	1.08	1.08
	Interatomic Angles (deg)	
$C_2-C_1-S_5$	111.54	112.33
$C_2-C_1-H_9$	126.90	126.46
$S_5-C_1-H_9$	121.56	121.21
$C_2-C_3-S_4$	112.48	113.90
$O_7-C_6-O_8$	122.23	129.68
	Dihedral Angles (deg)	
$S_5-C_1-C_2-C_3$	0.0	0.0
$S_5-C_1-C_2-C_6$	180.0	180.0
$C_3-C_2-C_6-O_8$	0.00	180.0

of the neutral molecule is estimated to be −15.03 eV, which is more stable than the anionic form of the molecule. The corresponding energies at the global minima of the potential energy surfaces of 3-TCA and 3-TCA$^-$ are ∼−20184.172 eV and ∼ −20169.139 eV, respectively. Table 1 shows the selected optimized structural parameters of two different forms of the molecule. To the best of our knowledge, no X-ray crystallographic, electron diffraction, or microwave data of the molecule has yet been established. However, the theoretical results as obtained from the DFT calculations are almost comparable with the reported structural parameters of the parent thiophene molecule.[25]

The theoretically simulated distribution of the microspecies and the variation in charge of the molecule with pH are shown in panels a and b of Figure 2, respectively. The −COOH functional group of the 3-TCA molecule has a pK_a value of ∼3.56, and the isoelectric point of the molecule approximately spans over a wide range of pH between 0 and 3. Thus, except at moderate to extreme acidic pH (<4) values; the molecule exists as the anionic form.

4.2. Normal Raman and FTIR Spectra of the Molecule and Their Vibrational Assignment. The 3-TCA molecule and its anionic form (3-TCA$^-$) have 12 and 11 atoms, respectively. Hence, the 3-TCA molecule has 30 fundamental vibrations that are distributed among the symmetry species as $\Gamma_{vib} = 21A' + 9A''$. The 3-TCA$^-$ form of the molecule, on the other hand, has 27 normal modes of vibrations which are classified as $\Gamma_{vib} = 19A' + 8A''$. Both the neutral and the anionic form of the molecule belong to C_s point group symmetry. Hence, the 30 and 27 fundamental vibrations of the neutral and the anionic forms of the molecule are expected to appear both in the Raman and in the FTIR spectra. However, among these vibrations, some normal mode/modes may emanate either from the neutral form (3-TCA), from the anionic form (3-TCA$^-$), or from both the forms of the molecule, signifying the possibility of some vibrational signatures to be degenerative.

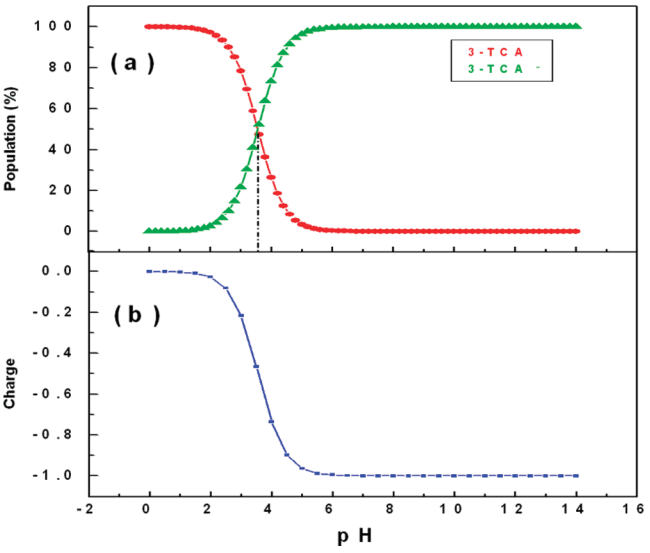

Figure 2. (a) Distribution of microspecies with pH. (b) Variation in charge of the molecule with pH.

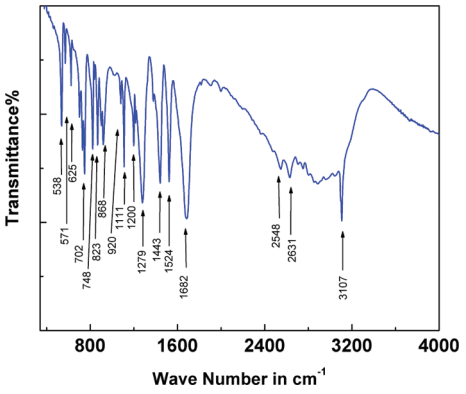

Figure 3. FTIR spectrum of the molecule of neat powder in a KBr pellet.

The FTIR spectrum of neat powder in a KBr pellet is presented in Figure 3. The recorded NRS spectra of the molecule in neat solid and in 0.1 M ACN solution at neutral pH (∼7.0) are shown in panels a and b of Figure 4, respectively. Panels c and d of Figure 4 show the theoretically simulated NRS spectra of the 3-TCA and the 3-TCA$^-$ forms of the molecule in the gas phase, respectively. The underlying aim of recording the FTIR and NRS spectra is to apprehend the existence of the preferential form/forms of the molecule in the solid state and in ACN solution after assigning the vibrational signatures.

Table 2 lists the experimentally observed FTIR and NRS band frequencies of the molecule. The theoretically computed vibrational frequencies of the neutral and the anionic forms of the molecule in the gas phase are also shown in Table 2 along with their tentative assignments, as provided by the potential energy distribution (PED) calculation. The PEDs have been estimated in terms of the internal coordinates of the molecule, from the output of the DFT calculations. The observed disagreement between the theory and the experiment could be a consequence of the anharmonicity and may be due to the general tendency of the quantum chemical methods to overestimate the force constants at the exact equilibrium geometry. However, it is to be

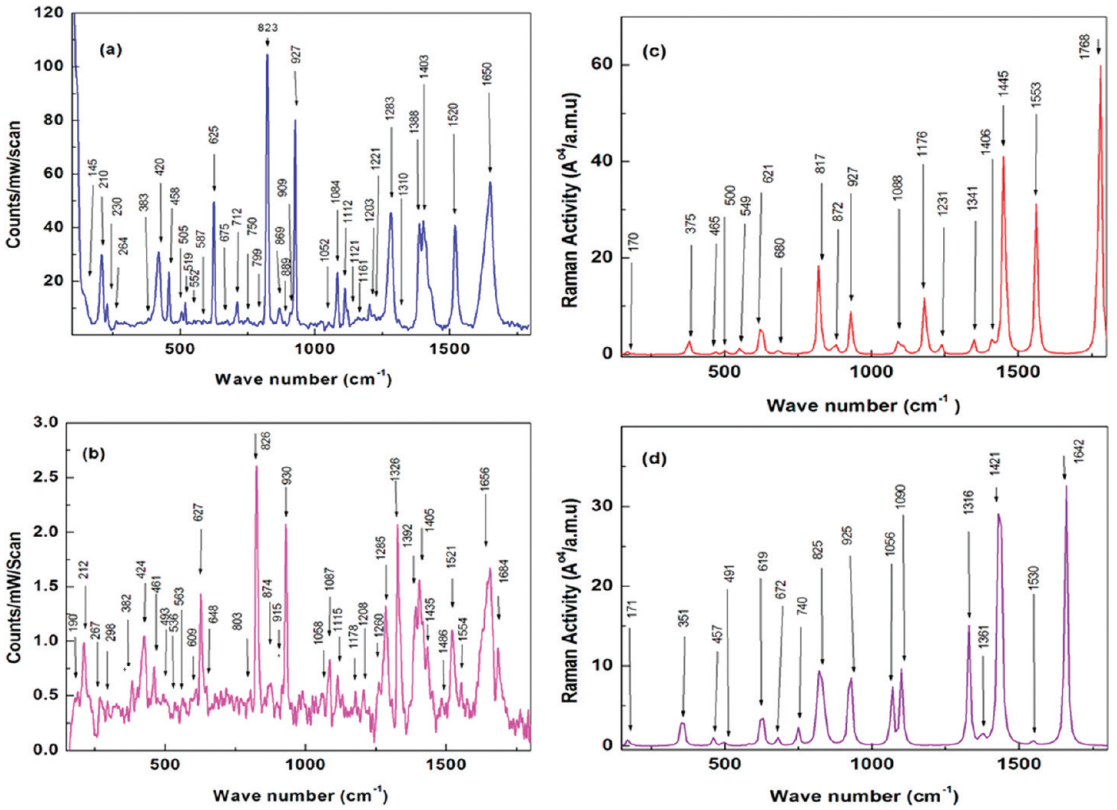

Figure 4. (a and b) Normal Raman spectra of the molecule in (a) the solid state or (b) 0.1 M acetonitrile solution (λ_{exc} = 514.5 nm). (c and d) Theoretically simulated gas-phase Raman spectra of the (c) 3-TCA and (d) 3-TCA$^-$ forms of the molecule calculated using DFT. Asterisks denote the solvent ACN bands.

emphasized that the calculated Raman spectrum represents the vibrational signatures of molecules in the gas phase. Hence, the experimentally observed NRS of solid and solution may differ significantly from the calculated spectrum. Despite this fact, one can see that there is a general concordance regarding the Raman intensities as well as the positions of the peaks between the experimental and calculated spectra.[26,27]

The FTIR spectrum of the powdered sample (Figure 3) and the NRS spectrum of the molecule in the solid state (Figure 4a) are characterized by sharp and well-resolved vibrational bands. However, some of the vibrational signatures, particularly in the higher wavenumber region of the IR and NRS spectra appear as broad and structureless. Compared to the NRS spectrum of the molecule recorded in the solid state, the spectrum of the molecule in ACN solution at neutral pH ~7 (Figure 4b) exhibits almost the same nature of the Raman bands. The modes arising principally from the torsion, stretching, and bending vibrations of the thiophene ring moiety of both the anionic and the neutral forms of the molecule are identified. In assigning the vibrational frequencies, literature concerning the normal coordinate analysis and vibrational assignments of the thiophene as well as related molecules has been considered.[28] The NRS spectra of the molecule, recorded both in the solid state and in ACN solution are characterized by intense, jagged, and well-resolved bands centered at ~625, 823, and 927 cm^{-1} whose calculated values are 927/916 cm^{-1}, 624/619 cm^{-1}, and 817/825 cm^{-1} for the 3-TCA/3-TCA$^-$ forms of the molecules respectively. Except for the band at ~625 cm^{-1}, the 823 and 927 cm^{-1} bands also exhibit moderate absorbance in the IR spectrum. All the above-mentioned bands are ascribed to the in-plane bending vibrations emanating either from 3-TCA/3-TCA$^-$ or from both the forms of the molecule. This experimental result primarily indicates the presence of both the neutral and the anionic forms of the molecule in the solid state and in ACN solution. The NRS spectra of the molecule recorded in the solid state and in ACN solution as shown in parts a and b of Figure 4, respectively, apparently look similar. However, deeper introspection of the NRS spectra of the molecule recorded in the solid state and in ACN solution reveals some qualitative differences between the two.

For example, the moderately intense Raman band centered at ~457 cm^{-1} (calcd at 465/457 cm^{-1} for the 3-TCA/3-TCA$^-$ forms of the molecule) in the NRS spectrum of the molecule recorded in the solid state appears as a weak but distinct signal at ~458 cm^{-1} in the ACN solution. This band has a significant contribution arising from the torsion of the thiophene ring moiety of the 3-TCA and/or its anionic 3-TCA$^-$ form of the molecule. The appearance of this normal mode in the NRS spectrum further suggests the presence of both the forms (3-TCA and 3-TCA$^-$) in the solid state as well as in the ACN solution. This result is in accordance with our earlier conjecture (vide supra). The presence of both the neutral and the anionic forms of the molecule in the solid state is further corroborated by the appearance of a strong band at ~748 cm^{-1} (calcd at 767 cm^{-1} for 3-TCA and at 758 cm^{-1} for the 3-TCA$^-$ forms of the molecule), in the FTIR spectrum. This band appears as a weak signal in the NRS spectrum of the molecule recorded in the solid state and disappears in ACN solution. Generally, the out-of-

plane modes show strongly in the infrared and weakly in the Raman, and the band is assigned to have the prevailing contribution from the out-of-plane γ ($H_9-C_1-S_5-C_2$) vibrations emanating from the 3-TCA and 3-TCA$^-$ forms of the molecule.

Interesting observations can be drawn regarding the appearance of a strong and well resolved band at ~1403 cm^{-1} (calcd at 1406 cm^{-1}) for 3-TCA in the NRS spectra of the molecule recorded in the solid state and in ACN solution, whose IR counterpart shows a very weak hump at ~1406 cm^{-1}. This band has been ascribed to have a predominant contribution from the stretching $\nu(C_2-C_3)$ as well as the in-plane $\alpha(S_5-C_1-H_9)$ and $\alpha(C_6-0_8-H_{12})$ bending vibrations descending from the 3-TCA form of the molecule. This observation may thereby specifically portend the presence of the 3-TCA form of the molecule both in the solid state and in ACN solution. However, the presence of the 3-TCA form of the molecule in the solid state is corroborated by the appearance of a strong band at ~728 cm^{-1} (calcd 710 cm^{-1}), in the FTIR spectrum. This band has been ascribed to the torsional vibrations of the thiophene ring moiety emanating from the 3-TCA form of the molecule.

Interestingly, the presence of the 3-TCA$^-$ form of the molecule both in the solid state and in ACN solution can also be envisaged from the vibrational signatures recorded at ~1431 and at ~1522 cm^{-1}. The band at ~1431 cm^{-1} (calcd 1421 cm^{-1}) for the 3-TCA$^-$ form shows strong absorbance in the FTIR spectra, and the NRS counterpart recorded in the solid state and in solution shows weak and medium strong intensity, respectively. The other band at ~1522 cm^{-1} (calcd 1530 cm^{-1}) appears as a strong signal both in the FTIR and in the NRS. Both the above-mentioned vibrational signatures have been ascribed to have a dominant contribution from the stretching and in-plane bending modes arising from the 3-TCA$^-$ form of the molecule.

Considerable attention can be drawn regarding the band centered at ~1650 cm^{-1} (calcd 1642 cm^{-1}), which appears as broad and intense signal in the NRS spectrum of the molecule recorded in the solid state and in ACN solution. This band in the NRS spectrum of the molecule in ACN solution exhibits a more structured pattern, in comparison with that recorded in the solid state. This is evidenced by the appearance of weak kinks and shoulders around the intense band centered at ~1654 cm^{-1}. The band has been ascribed to have a prevailing contribution from the carbonyl stretching and in-plane $\alpha(C_1-C_2-C_6)$; $\alpha(C_3-C_2-C_6)$ bending vibrations, emanating from the 3-TCA$^-$ form of the molecule. This observation indicates the presence of the 3-TCA$^-$ form of the molecule in ACN solution.

Significant conclusions can be drawn regarding the appearance of a very strong band for the 3-TCA$^-$ form at ~1326 cm^{-1} (calcd ~1316 cm^{-1}) in the NRS spectrum of the molecule recorded in ACN solution. This band is absent both in the FTIR and in the NRS spectrum of the molecule recorded in the solid state. The band has been ascribed to have a significant contribution from the $\nu(C_6{=}O_7)$ stretching and in-plane $\alpha(S_5-C_4-H_{11})$; $\alpha(C_3-C_4-H_{11})$ bending vibrations descending from the 3-TCA$^-$ form of the molecule. The vibrational signature at ~1326 cm^{-1}, recorded only in the NRS spectrum in solution, may be considered as a marker band and corroborates the presence of the 3-TCA$^-$ form of the molecule in the ACN solution.

The vibrational analysis of the experimentally observed FTIR and the NRS spectra of the molecule aided by the DFT calculations thus helps us to identify the marker bands representing vibrational signatures descending from the neutral form, the anionic form, or both the forms of the molecules in the solid state and in ACN solution. The concomitance of the Raman bands representing vibrational signatures emanating from the neutral and the anionic forms of the molecules may signify the presence of both the forms of the molecule. The appearance/disappearance of certain Raman bands together with the variation in intensities of the Raman bands in the NRS spectra of the molecule recorded in the solid state and in ACN solution may portend variations in the respective population of the neutral/anionic forms of the molecule in the solid state and in solution.

However, the respective population of the neutral/anionic forms of the molecule may vary in the solid state and in ACN solution.

The quantitative measure of relative population of the neutral and the anionic forms in the solid state and in ACN solution can be estimated from the ratio of the sum of the integrated intensities of the assigned experimental bands, representing vibrational signatures of the molecules divided by the theoretically predicted sums of the absolute intensities of the respective bands.[29] The relative population of the two forms of the molecule can be evaluated as follows by eq 1.

$$\frac{[\text{3-TCA}]}{[\text{3-TCA}^-]} = \frac{\sum I^{\text{3-TCA}} \sum A^{\text{3-TCA}^-}}{\sum I^{\text{3-TCA}^-} \sum A^{\text{3-TCA}}} \quad (1)$$

where I and A are the integrated and absolute intensities of the molecules, respectively.

Figure 5 shows the bar diagram indicating the relative population of the neutral and the anionic forms of the molecule in the solid state and in ACN solution. The results indicate that 54% of the neutral form (3-TCA) of the molecule is prevalent in the solid state while 63% of the anionic form (3-TCA$^-$) of the molecule predominates in ACN solution at neutral pH. This result is in accordance with our earlier conjecture as predicted from the vibrational assignment (vide supra).

4.3. Concentration Dependent and pH Dependent SERS Spectra of the Molecule. Figure 6 shows that the normalized SERS spectra of the molecule at varied C_{Ad} are characterized by a number of sharp and well-resolved Raman bands. The 921 cm^{-1} band of ACN is moderately intense in the entire concentration dependent SERS spectral profile, and hence, all the SERS spectra of the molecule recorded at various C_{Ad} have been normalized with respect to this band for visual clarity. It is established from the previous reports that ACN does not show surface enhancement in silver nanocolloid;[30] thus, any possible interaction of ACN with silver nanocolloid can be neglected.

Figure 7 shows the variation of the normalized intensity of the SERS signals of the 1649, 1362, 1508, 1308, 611, and 771 cm^{-1} bands with the logarithm of C_{Ad}. It is observed that the overall SERS signal of the molecule attains a maximum value at C_{Ad} = 1.0×10^{-2} M and then decreases with further decrease in C_{Ad}. It is now well established that, both on silver-island films[31] and in nanocolloid,[32] maximum enhancement is observed when a monolayer of the adsorbate molecule is formed on the surface and the SERS signal decreases when multilayers or submonolayer is formed. At extremely low C_{Ad}, the nanocolloidal surface embraced by the adsorbate is submonolayer, and in the absence of sufficient scattering molecules, the SERS signal is weak. With an increase in C_{Ad}, the surface coverage increases, and the SERS signal increases and attains a maximum intensity on C_{Ad}, where both the EM and CT contributions to SERS maximize. On further increase of C_{Ad}, the multilayers are formed and the SERS

Table 2. Observed and Calculated IR and Raman Bands of the Molecule in Varied Environments and Their Tentative Assignments[a]

FTIR (obs)	NRS solid	NRS in solution	symmetry species	theoretical Raman 3-TCA^0	assignment (PED)%	theoretical Raman 3-TCA^{-1}	assignment (PED)%
	145w/sh	187w	A″	170	$54(\tau_{1,2,3,4};\ \tau_{6,2,3,4};\ \tau_{1,2,3,10};\ \tau_{6,2,3,10})\ 35\gamma_{6,2,1,3}\ 6\gamma_{9,1,2,5}$	171	$45\tau_{6,2,1,3}\ 21(\tau_{1,2,6,7};\ \tau_{3,2,6,7};\ \tau_{1,2,6,8};\ \tau\Gamma_{3,2,6,8})\ 16\tau_{9,1,2}\ 6\tau_{10,3,2,4}\ 6\tau_{ring}$
	210ms	210ms	A′	192	$98\alpha_{3,2,6}$	185	$96(\alpha_{1,2,6};\ \alpha_{3,2,6})$
			A′	375	$24(\alpha_{6,8,12};\ \alpha_{2,3,10})\ 21\alpha_{1,2,6}\ 10\alpha_{5,4,11}\ 9(\alpha_{5,1,2};\ \alpha_{1,2,3};\ \alpha_{4,5,1};\ \alpha_{2,3,4})$	351	$37(\alpha_{5,1,9}\ ;\ \alpha_{2,1,9})\ 29(\alpha_{2,3,10};\ \alpha_{4,3,10})\ 13(\alpha_{5,1,2};\ \alpha_{1,2,3}\ \alpha_{4,5,1};\ \alpha_{3,4,5})\ 11(\alpha_{1,2,3};\ \alpha_{4,5,1};\ \alpha_{2,3,4};\ \alpha_{3,4,5})\ 7(\alpha_{5,4,11};\ \alpha_{3,4,11})$
	419ms	423	A′		$10\alpha_{5,4,11}\ 9(\alpha_{5,1,2};\ \alpha_{1,2,3};\ \alpha_{4,5,1};\ \alpha_{2,3,4})$		
	457ms	458w	A″	465	$83\tau_{ring}\ 11\tau_{6,2,1,3}$	457	$40(\tau_{5,1,2,3};\ \tau_{4,5,1,2};\ \tau_{1,2,3,4};\ \tau_{3,4,5,1};\ \tau_{2,3,4,5})\ 24(\tau_{1,2,7,9};\ \tau_{3,2,6,7};\ \tau_{1,2,6,8};\ \tau_{3,2,6,8})\ 8\tau_{11,4,5,3}\ 7\tau_{ring}\ 7\ \gamma_{10,3,4,2}\ 7\gamma_{6,2,1,3}\ 6\gamma_{9,1,2,5}$
	504ms	497vw	A′	500	$80(\alpha_{3,2,6};\ \alpha_{1,2,6})\ 13\alpha_{2,3,10}$	491	$90(\alpha_{1,2,6};\ \alpha_{6,2,3})\ 5(\alpha_{2,1,9};\ \alpha_{5,1,9})$
571w			A″	549	$66(\tau_{7,6,8,12};\ \tau_{2,6,3,12})\ 33\tau_{ring}\ 6\tau_{6,2,1,3}$	576	$55\tau_{ring}\ 19\gamma_{6,2,3,1}\ 14\gamma_{11,4,5,3}$
626w	625s	624s	A′	621	$33\alpha_{2,3,10}\ 20\alpha_{6,8,12}\ 15(\alpha_{3,4,11};\ \alpha_{5,4,11})\ 10(\alpha_{5,1,2};\ \alpha_{1,2,3};\ \alpha_{ring})\ 8(\alpha_{2,1,9};\ \alpha_{5,1,9})\ 6(\alpha_{1,2,3};\ \alpha_{4,5,1})$	619	$72(\alpha_{3,4,5};\ \alpha_{5,1,2};\ \alpha_{4,3,1};\ \alpha_{2,3,4})\ 17(\alpha_{2,1,9};\ \alpha_{5,1,9})$
			A″	626	$70(\tau_{2,6,8,12};\ \tau_{12,8,6,7})\ 12\tau_{6,2,3,1}\ 8(\tau_{1,2,3,10};\ \tau_{6,2,3,10})\ 7\tau_{ring}$		
			A″/A′	680	$35\alpha_{6,8,12}\ 20\gamma_{6,8}\ 18(\alpha_{2,3,10};\ \alpha_{4,3,10})\ 14(\alpha_{2,1,9};\ \alpha_{5,1,9})\ 7\alpha_{1,2,6}$	672	$59\gamma_{11,4,5,3}\ 17\gamma_{10,3,2,4}\ 16\gamma_{9,1,5,2}$
704w	710w	712vvw	A″/A′	710	$37\gamma_{11,4,3,5}\ 27(\tau_{6,2,3,10};\ \tau_{1,2,3,10})\ 27\gamma_{9,1,5,2}\ 6\tau_{10,3,2,4}$	740	$42(\alpha_{2,3,10};\ \alpha_{4,3,10})\ 21(\alpha_{3,2,6};\ \alpha_{1,2,6})\ 12(\alpha_{2,1,9};\ \alpha_{5,1,9})$
748vs	750vw		A′				$11(\alpha_{1,2,3};\ \alpha_{4,5,1};\ \alpha_{2,3,4};\ \alpha_{3,4,5})\ 11(\alpha_{5,4,11};\ \alpha_{3,4,11})$
			A″	767	$58\gamma_{9,1,2,5}\ 23(\tau_{2,6,8,12};\ \tau_{1,6,8,12})\ 14\gamma_{6,2,1,3}$	758	$76\gamma_{9,1,5,2}\ 13\gamma_{10,3,4,2}\ 5\gamma_{11,4,5,3}$
			A′			809	$46(\alpha_{1,2,3};\ \alpha_{4,5,1};\ \alpha_{3,2,4};\ \alpha_{3,4,5}\ 23(\alpha_{2,3,10};\ \alpha_{4,3,10})\ 19\ (\alpha_{2,1,9};\ \alpha_{5,1,9}\ 11(\alpha_{3,2,6};\ \alpha_{1,2,6})$
824ms	824ms	825vvs	A′	817	$86(\alpha_{2,3,10};\ \alpha_{4,3,10})$	825	$49(\alpha_{2,1,9};\ \alpha_{5,1,9})\ 31(\alpha_{1,2,6};\ \alpha_{3,2,6})\ 10(\alpha_{2,3,10};\ \alpha_{4,3,10})$
868ms			A″	851	$68\gamma_{9,1,8,5}\ 16\gamma_{6,8,1,3}\ 9\tau_{ring}$	845	$63\gamma_{9,1,2,5}\ 20\gamma_{6,2,1,3}\ 8\gamma_{11,4,3,5}$
902ms							
			A″	920	$54\gamma_{10,3,4,2}\ 25\gamma_{11,4,5,3}\ 13\tau_{ring}$	925	$80\gamma_{10,3,4,2}\ 6\gamma_{11,4,3,5}\ 6\tau_{ring}$
921ms	927vs	929vs	A′	927	$88\alpha_{5,4,11}\ 6\gamma_{6,8}$	916	$64(\alpha_{5,4,11};\ \alpha_{3,4,11})\ 31(\alpha_{1,2,3};\ \alpha_{11,4,5};\ \alpha_{4,5,1};\ \alpha_{3,4,5})$
	1052vw	1056vw	A′			1056	$43(\alpha_{2,1,9};\ \alpha_{5,1,9})\ 37(\alpha_{2,3,10};\ \alpha_{4,3,10})\ 20(\alpha_{5,4,11};\ \alpha_{3,4,11})$
1080w	1084ms	1088vw/sh					
			A′	1088	$68(\alpha_{2,3,10};\ \alpha_{4,3,10})\ 18(\alpha_{2,1,9};\ \alpha_{5,1,9})\ 11\ (\alpha_{3,4,11};\ \alpha_{5,4,11})$	1090	$48(\alpha_{2,1,9};\ \alpha_{5,1,9})\ 38(\alpha_{5,4,11};\ \alpha_{3,4,11})\ 14(\alpha_{2,3,10};\ \alpha_{4,3,19})$
1112vs	1112w	1113w	A′	1106	$49(\alpha_{2,3,10};\ \alpha_{3,4,11})\ 46(\alpha_{5,4,11};\ \alpha_{3,4,11})$		
	1121vw	1129w					
	1161vvw						
		1178vvw	A′	1176	$44\alpha_{6,8,12}\ 26(\alpha_{2,1,9};\ \alpha_{5,1,9})\ 18(\alpha_{3,4,11};\ \alpha_{5;4;11})\ 8\gamma_{6,8}$		
1203 ms	1204vw	1205w	A′			1190	$37(\alpha_{2,1,9};\ \alpha_{5,1,9})\ 33(\alpha_{5,4,11};\ \alpha_{3,4,11})\ 25(\alpha_{2,3,10};\ \alpha_{4,3,10})$
1220w	1221vw		A′	1231w	$65(\alpha_{2,3,10};\ \alpha_{4,3,10})\ 23(\alpha_{3,4,11};\ \alpha_{5,4,11})\ 9(\alpha_{2,1,9};\ \alpha_{5,1,9})$		
1280vvs	1283s	1283s					
		1304w					
		1325vs	A′			1316	$65\nu_{6,7}\ 26(\alpha_{5,4,11};\ \alpha_{3,4,11})$
			A′	1341	$43\alpha_{6,8,12}\ 32(\alpha_{2,3,10};\ \alpha_{4,3,10})\ 13(\alpha_{3,4,11};\ \alpha_{5,4,11})$		
			A′			1361	$56(\alpha_{5,4,11};\ \alpha_{3,4,11})\ 21(\alpha_{2,3,10};\ \alpha_{4,3,10})\ 19(\alpha_{2,1,9};\ \alpha_{5,1,9})$
		1390s					
1406w	1403s	1403s	A′	1406	$61\nu_{2,3}\ 23(\alpha_{5,1,9};\ \alpha_{2,1,9})\ 12\alpha_{6,1,12}$		
1435s	1431w/sh	1430 ms/sh	A′			1421	$64\nu_{C=C}\ 14\alpha_{2,3,10}\ 11\alpha_{3,4,11}\ 7\alpha_{2,1,9}$
		1450w/sh	A′	1445	$85\nu_{C=C}\ 10\alpha_{6,8,12}$		
		1482vvw					
1522s	1517s	1520s	A′			1530	$67\nu_{C=C}\ 16\alpha_{4,3,10}\ 9\alpha_{3,4,11}\ 7\alpha_{2,1,9}$
		1553vw	A′	1553	$77\nu_{C=C}\ 12(\alpha_{2,3,10};\ \alpha_{4,3,10})\ 6(\alpha_{5,1,9};\ \alpha_{2,1,9})$		
		1574vvw					

dx.doi.org/10.1021/jp204297y | J. Phys. Chem. C 2011, 115, 14309–14324

Table 2. Continued

FTIR (obs)	NRS solid	NRS in solution	symmetry species	theoretical Raman 3-TCA^{0}	assignment (PED)%	theoretical Raman 3-TCA^{-1}	assignment (PED)%
		1608w/k					
		1618w/sh					
		1630ms/sh					
		1645w/sh	A′			1642	$65\nu_{C=Oo}$ $31(\alpha_{1,2,6}; \alpha_{3,2,6})$
	1650s/br	1654s					
1680vvs/br		1683w					
			A′	1768	$85\nu_{6,7}$ $12\alpha_{6,8,12}$		
2546w							
2628w		2625w					
		2649s					
2701w		2702vvw/br					
		2792vw					
2803vw		2806w					
2855vw		2862w/br					
2971vvw/br							
	3023w						
3051vw/br	3051w						
		3070w					
3097w/k	3094s/k	3097vvw/k					
3109s	3112vvs	3112w					
			A′			3171	$91\nu_{4,11}$
			A′			3192	$99\nu_{4,11}$
			A′	3208	$80\nu_{3,10}$ $11\nu_{4,11}$		
			A′			3216	$92\nu_{1,9}$
			A′/A″	3233	$86\nu_{4,11}$ $10\gamma_{3,10}$		
			A′	3239	$88\nu_{1,9}$		
		3469ms					
		3479vvs					
		3589ms					
	3707vw	3704ms					
			A′	3728	$96\nu_{8,12}$		
		3731vw					
		3753s					
	3913vw	3908vvw					
		3935vvw					

[a] vs, very strong; s, strong; ms, medium strong; w, weak; vw, very weak; vvw, very very weak; sh, shoulder; br, stretching; α, in-plane bending; γ, out-of-plane bending; τ, torsion; contributions $\geq$ 5 are reported only.

dx.doi.org/10.1021/jp204297y | J. Phys. Chem. C 2011, 115, 14309–14324

signal decreases in intensity. It therefore seems plausible that the monolayer of the molecule may have formed on the silver nanocolloidal particles at $C_{Ad} = 1.0 \times 10^{-2}$ M, which shows maximum enhancement of the overall SERS signal. The above experimental results as shown in Figures 6 and 7 mark the presence of free molecules in solution, and the ratio of the free-to-bound molecules on the nanocolloidal silver surface changes with $C_{ad.}$ Recently, the ratiometric SERS quantification method has been successfully utilized[33] for quantifying the adsorption of the probe molecule on the nanocolloidal surface. In a separate publication, the method will be applied to estimate the ratio of the free to bound molecules at various C_{ad}.

Considerable attention can be drawn regarding the intense band centered at ~1362 cm^{-1} in the SERS spectra of the molecule recorded at various C_{Ad} values (Figure 6). This band is considerably red-shifted with respect to its NRS counterpart, which appears as a strong signal at ~1388 cm^{-1} (calcd at 1341 cm^{-1} for 3-TCA and 1361 cm^{-1} for 3-TCA^-). The band has been ascribed to have an intervening contribution from the in-plane bending vibration of the thiophene ring moiety of the molecule originating from the 3-TCA and/or 3-TCA^- forms of the molecule. Similar shifting is also observed for the SERS band centered at ~611 cm^{-1}, which is considerably red-shifted with respect to its NRS counterpart peaked at ~624 cm^{-1}. The band has a significant contribution from the in-plane bending vibration involving both the oxygen (O_8) and/or sulfur (S_5) atom of the 3-TCA and 3-TCA^-, respectively. The red shift may signify the involvement of the O_8 and/or S_5 atom/atoms of the 3-TCA or 3-TCA^- or both the forms of the molecule in the adsorption process with the nanocolloidal silver surface. The appearance of flexes and shoulders in the frequency range 150−180 cm^{-1} and at ~225 cm^{-1} in the entire concentration dependent SERS profile is ascribed to the Ag−S_5[34] and Ag−O[35] stretching vibrations, respectively. This observation indicates that the molecule is indeed adsorbed through the lone pair electron of the sulfur (S_5) and oxygen atoms via σ bond formation.

However, the entire concentration dependent SERS spectral profile of the molecule is epitomized by the Raman bands centered at ~1308 and 1508 cm^{-1}. Both these bands are considerably red-shifted with respect to their corresponding NRS counterpart centered at ~1326 cm^{-1} (calcd ~1316 cm^{-1}) and 1520 cm^{-1} (calcd 1530 cm^{-1}) for the 3-TCA^- form in ACN solution, respectively. The former band has been ascribed to have a significant contribution from the C_6═O_7, while the latter is assigned to have a dominant contribution from the C═C stretching vibration, both emanating from the anionic form of the molecule. The red shift of the above-mentioned bands in the SERS spectra of the molecule not only signifies the involvement of the π electron cloud localized in the thiophene ring and in the carbonyl group of the molecule but also smears the preponderance of the anionic (3-TCA^-) form in the surface adsorbed state. The downshift of the above-mentioned bands in the SERS spectra of the molecule may be envisioned by considering the donation of electron density from the π electron cloud localized in the thiophene ring moiety and in the carbonyl group of the molecule to the s-orbital of the metal in the nanocolloid. It is then followed by the back-donation of the electron density from the s-orbital of the metal to the conduction band (ca. vacant π^* antibonding orbitals) of the thiophene ring and carbonyl group of the molecule. This process leads to the weakening of the C_6═O_7 and C═C double bonds, resulting in red shift of their respective vibrational frequencies. The substantial red shift of the stretching

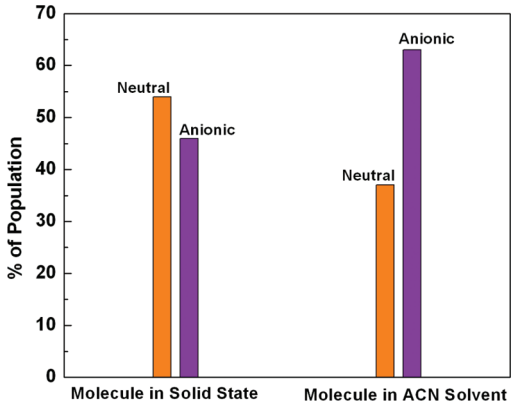

Figure 5. Bar diagram indicating the relative percentage population of the neutral (ca. 3-TCA) and the anionic (ca. 3-TCA^-) forms of the molecule.

vibrations of the molecules involving a thiophene ring moiety is a general observation and has been reported in the literature.[34] The presence of the 3-TCA^- form of the molecule in the surface adsorbed state is further corroborated by the appearance of a sharp and intense band at ~1650 cm^{-1} in the SERS spectra of the molecule recorded at various C_{Ad} values. This SERS band though has a different band profile; however, its corresponding NRS counterpart appears almost in the same position as that in the SERS. Absence or weak involvement of the neutral (3-TCA) form of the molecule in the surface adsorbed state may be envisaged by considering the absence of the SER bands ~1403 cm^{-1} and ~728 cm^{-1} ascribed to the in-plane and out-of-plane vibrations respectively emanating from the neutral form of the molecule. An interesting conclusion can be drawn regarding the band centered at ~771 cm^{-1}, which appears as broad and moderately intense signal in the entire concentration dependent SERS spectra of the molecule. This band may have its NRS counterpart at ~748 cm^{-1} (calcd at 767/758 cm^{-1} for the 3-TCA/3-TCA^- forms of the molecule) and has been ascribed to out-of-plane vibrations involving the sulfur (S_5) atom of the molecule. Substantial blue shift of the above-mentioned band in the SERS spectra of the molecule in comparison to its NRS counterpart again indicates the active involvement of the sulfur (S_5) atom of the molecule in the adsorption process, as predicted in our earlier conjecture.

In this connection, it may be mentioned that the SERS spectra of thiophene molecules adsorbed on silver and gold electrodes divulge the oligomerization of the thiophene molecules at the electrode surfaces.[36] However, the rational proof pertaining to the oligomerization of the 3-TCA and/or 3-TCA^- forms of the molecules adsorbed on silver nanocolloids is not suggested. The SERS spectra of the molecule recorded at various C_{Ad} values (Figure 6) are characterized by a number of sharp, well resolved Raman bands, which are not in harmony with the broad vibrational signatures of the polythiophene molecules as reported elsewhere.[36] This result is also in accordance with the SERS spectra of isomeric formyl and methyl thiophene[34] molecules adsorbed on silver nanocolloids, where no traces of oligomerization of the respective molecules were suggested. The results of thin layer chromatography (TLC) also preclude the possibility of oligomeization of the molecule on the nanocolloidal surface.

Generalized two-dimensional correlation spectroscopy has been employed for further interpretation of the concentration

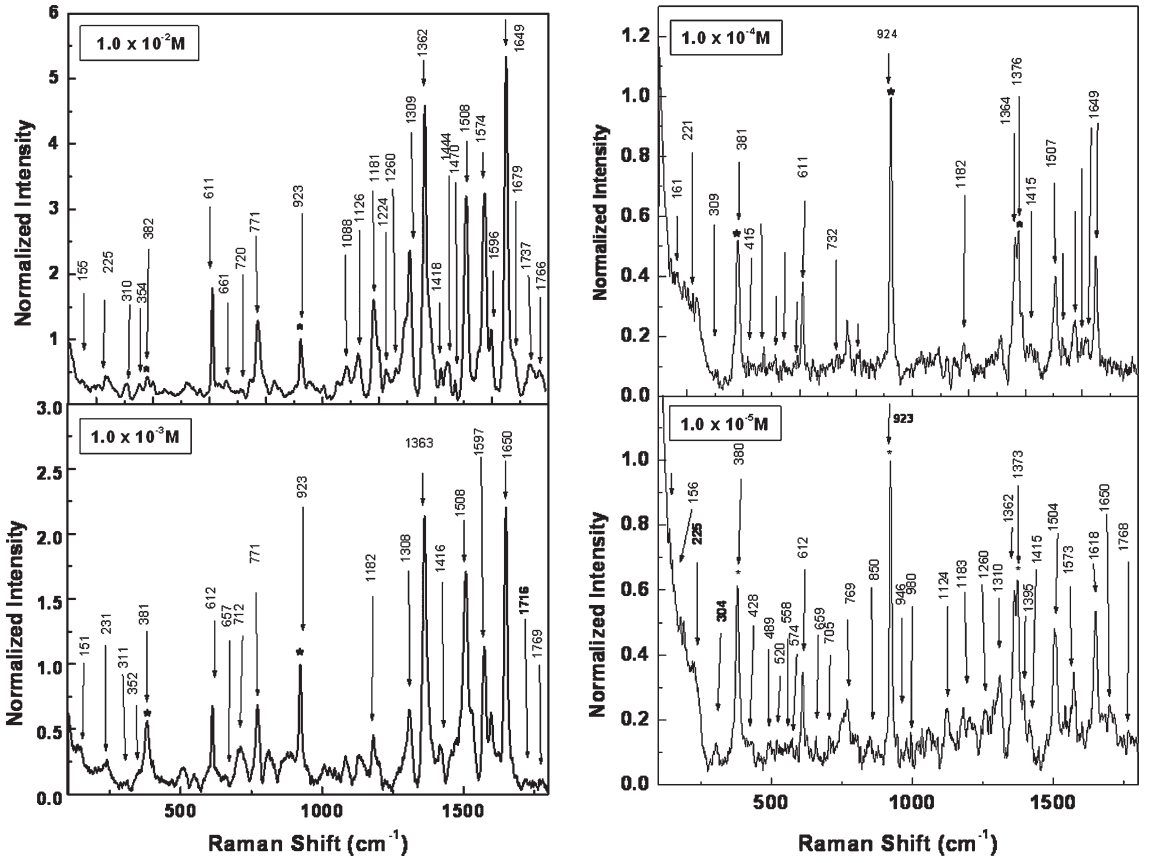

Figure 6. Normalized SERS spectra of the molecule at varied adsorbate concentrations (λ_{exc} = 514.5 nm).

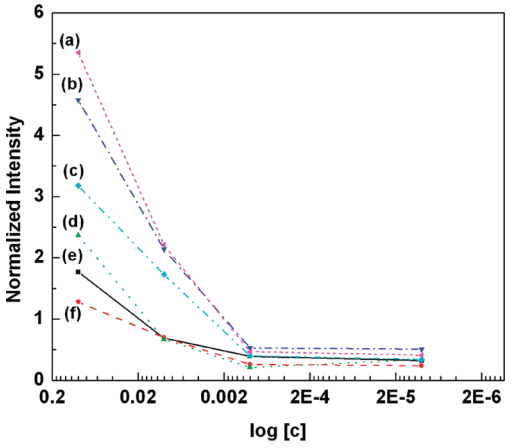

Figure 7. Concentration dependence of the intensity of the (a) 1649, (b) 1362, (c) 1508, (d) 1308, (e) 611, and (f) 771 cm^{-1} SERS bands of 2-ABT.

dependent SERS spectra of the molecule. Two-dimensional correlation spectroscopy (2D-COS) simplifies the investigation of complex spectra, enhancing spectral resolution by spreading peaks along the second dimension. This technique thus enables one to extract information that cannot be obtained from the conventional 1D spectrum.[37] The synchronous and asynchronous correlation spectra are generated from the 2D analysis. The synchronous spectra in the regions from 400 to 900 cm^{-1} and from 1250 to 1700 cm^{-1} are shown in Figure 8a. A synchronous spectrum is generally symmetric with respect to the diagonal line corresponding to coordinates $\nu_1 = \nu_2$. Any region of the spectrum that changes the intensity largely under a given perturbation will show strong autopeaks in the synchronous spectrum, while those remaining near constant develop little or no autopeaks. The presence of prominent autopeaks at ~611, 771, 1308, 1362, 1508, and 1650 cm^{-1} in the synchronous spectrum (Figure 8A) indicates that the intensity of these SERS bands undergoes changes largely under the change in the concentration of the adsorbate.

The asynchronous spectra (not shown) in the region do not show any traces of cross-peaks in the neighborhood of the SERS autopeak bands of the synchronous spectra. These results may indicate that the vibrational signatures at ~611, 771, 1308, 1362, 1508, and 1650 cm^{-1}, representing the SERS spectra of the molecule recorded at various C_{Ad} emanate exclusively from a particular form of the molecule in general and the anionic form ($3\text{-}TCA^-$) in particular. This may connote our earlier conjecture of the adsorption of the anionic form of the molecule on the nanocolloidal silver surface. The second derivative of the SERS spectra of the molecule at $C_{Ad} = 1.0 \times 10^{-2}$ M and 1.0×10^{-3} M shown in Figure 9A further endorses the presence of the 611, 771, 1308, 1362, 1508, and 1650 cm^{-1} bands, thereby substantiating the adsorption of the anionic form of the molecule in the surface adsorbed state.

The SERS spectra of the molecule at $C_{Ad} = 1.0 \times 10^{-2}$ M for various pH values of the nanocolloidal silver surface are shown in Figure 10. The spectra at various pH values are mainly subjugated by SERS bands centered at ~611, 771, 1308, 1362, 1508, and 1650 cm^{-1}. These bands are perceptible not only for large signal

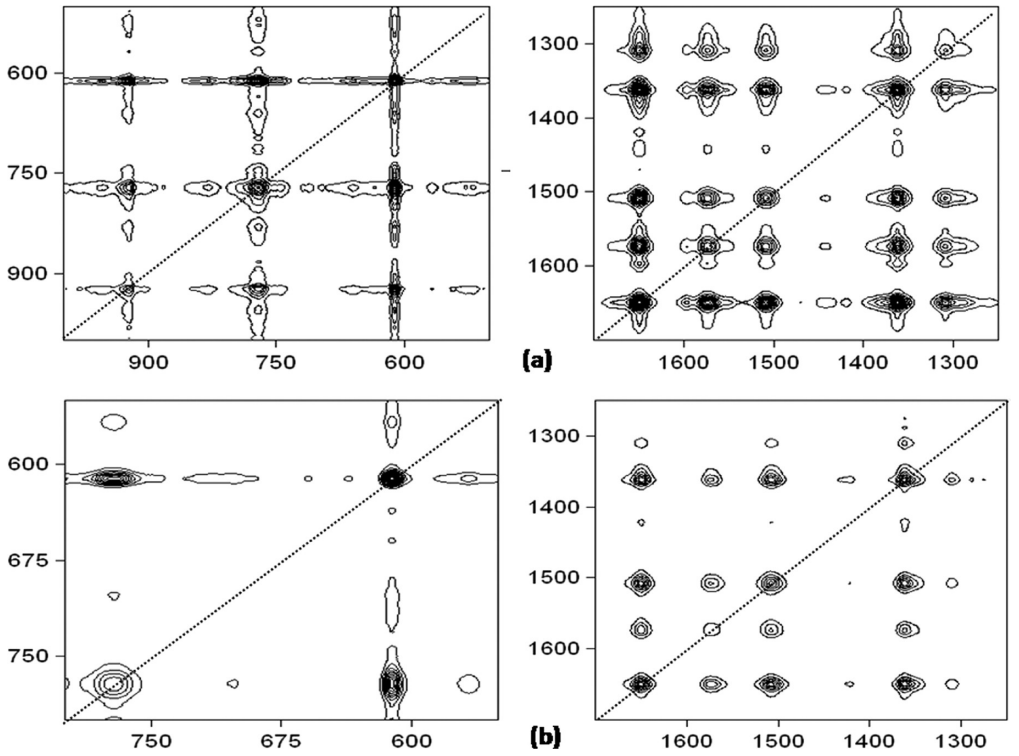

Figure 8. (a) Synchronous 2D correlation spectrum of the molecule in the ranges 400−900 cm^{-1} and 1300−1400 cm^{-1}, constructed from the concentration dependent SERS spectra. (b) Synchronous 2D correlation spectrum of the molecule in the ranges 400−900 cm^{-1} and 1300−1400 cm^{-1}, constructed from the pH dependent SERS spectra.

counts but also for interesting variations in the relative intensities with the variation in pH of the nanocolloidal silver surface. The full-width-at-half-maximum (fwhm) values of the above-mentioned SERS bands recorded at various pH values of the nanocolloidal silver surface are almost the same, and the 2D-COS resembles the identical synchronous contours and the asynchronous contours of the concentration dependent SERS spectra. The synchronous spectra, as obtained from the pH dependent SERS, in the regions from 400 to 900 cm^{-1} and from 1250 to 1700 cm^{-1}, are shown in Figure 8B. The appearance of the distinct Raman bands of the molecule, particularly at ∼1308, 1362, 1508, and 1650 cm^{-1} in the entire pH dependent SERS, and their corresponding second derivative spectral profile (Figure 9B) again indicate the adsorption of the anionic (3-TCA^-) form of the molecule on the nanocolloidal silver surface at acidic (pH ∼2, 4) and at neutral pH (∼7). This means that the molecule is ionized on the nanocolloidal surface even if the pH is much lower than that which is normally required to ionize the species. This may be due to considerably lower H^+ concentration near the nanocolloidal surface[38] as compared to the bulk solution, presumably because of the positive surface charge of the colloid. Alternatively, the Coulombic attraction may extend greater stability to the ionic form of the molecule near the nanocolloidal surface over the neutral species, which may effectively lower the pK_a value of the molecule.[39] Because the presence of no new band upon change of pH suggests structural changes of the molecule, the SERS spectral variations with pH may primarily be attributed to the orientational changes of the molecule.

4.4. Orientation of the 3-TCA^- Molecule on the Nanocolloidal Silver Surface. To have a precise idea regarding the orientation of the anionic form of the molecule at varied C_{Ad} values and various pH values of the solution, we estimate the apparent enhancement factors (AEFs) of some selected Raman bands by using eq 2, reported elsewhere.[4]

$$AEF = \sigma_{SERS}[C_{NRS}]/\sigma_{NRS}[C_{SERS}] \quad (2)$$

where C and σ represent the concentration and the peak area of the Raman bands measured from baseline. They are shown in Table 3. The orientation of the molecule has been estimated following the surface selection rule, as predicted by Moskovits.[40] According to this rule, the normal modes of the vibrations with the polarizability derivative components perpendicular to the surface will be enhanced more.

If the 3-TCA^- molecule is considered to be lying in the xy plane and z is perpendicular to the molecular plane, then for the edge-on adsorption, the vibrations of the in-plane (A′) species spanning as xx or yy (depending upon the stance of the molecule on the colloidal silver surface) are expected to undergo significant enhancement. For the face-on adsorption stance of the molecule on the nanocolloidal surface, the vibrations of the out-of-plane (A″) species transforming as yz and xz are expected to be enhanced. It is clearly seen from Table 3 that a moderate 2−4 orders of magnitude enhancement of almost all the SERS bands principally representing the in-plane vibrations of the A′ species of the 3-TCA^- molecule is recorded at various C_{Ad} values on the nanocolloidal silver surface. Moreover, the out-of-plane mode at around 771 cm^{-1}, belonging to the A″ symmetry species of the molecule, shows a significant (3.2×10^2 to 4.29×10^5) orders of magnitude enhancement. This is the lower limit of the enhancement factor by assuming that the largest possible value for the intensity of the NR line at ∼748 is equal to the noise.

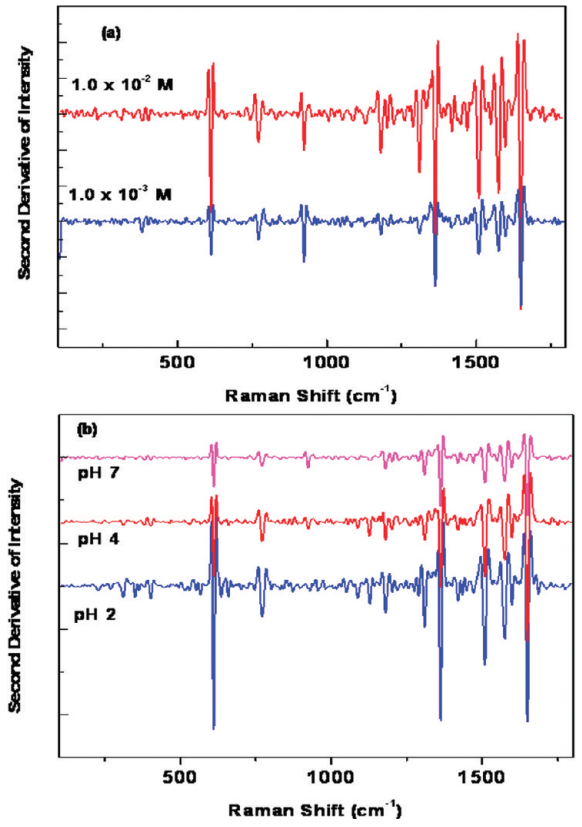

Figure 9. Second derivative SERS spectra of the molecule recorded (a) at various adsorbate concentrations and (b) at various pH values.

These results, together with the appearance of Ag−S_5, Ag−O stretching vibrations and disappearance of the in-plane vibrations at ∼826 and 930 cm^{-1} as well as the substantial red shifts of the 1308 and 1508 cm^{-1} bands in the SERS spectra with respect to their corresponding NRS counterparts, are important to understand the orientation of the molecule on the nanocolloidal silver surface. They suggest that the 3-TCA^- molecules are adsorbed onto the nanocolloidal silver surface through the S_5 and O atoms with the molecular plane tilted or nearly flat with respect to the nanocolloidal silver surface. The relative variation in intensities and enhancement factors of the SERS bands at various C_{Ad} values may indicate fluxional motion of the molecule on the nanocolloidal silver surface, yielding a distribution of tilted or nearly flat orientations.

A similar conclusion can be drawn regarding the orientation of the molecule adsorbed on the nanocolloidal silver surface having various pH values. The apparent enhancement factors of some selected SERS bands of the molecule adsorbed at various pH values of the nanocolloidal surface are shown in Table 3. The pH dependent SERS spectra of the molecule also suggest a tilted or nearly flat orientation of the molecule with respect to the nanocolloidal silver surface having acidic as well as neutral character. The relative variation in intensities and enhancement factors of the SERS bands at various pH values of the colloidal surface may again indicate fluxional motion of the molecule, as has been predicted from the concentration dependent SERS spectra.

4.5. CT Contribution to the SERS of the Molecule. In order to comprehend the selective enhancement of the vibrational signatures of the molecule belonging to A′ and A″ symmetry species in the SERS spectra of the molecule, the intensity of the

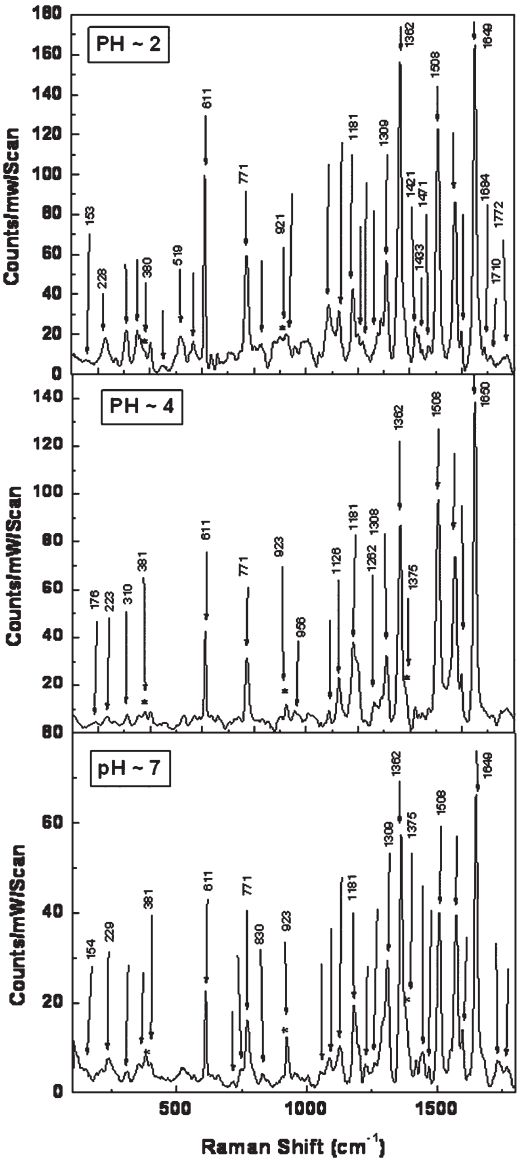

Figure 10. pH dependent SERS spectra of the molecule adsorbed on a silver nanocolloid at 1.0 × 10^{-2} M concentration (λ_{exc} = 514.5 nm).

Raman transition in terms of the polarizability tensor elements has been considered.

The intensity of the Raman transition is expressed by eq 3 as follows:

$$I = [8\pi(\omega \pm \omega_{I,I'})^4 I_L/9c^4]\sum\alpha_{\sigma\rho}^2 \quad (3)$$

where I_L is the incident laser intensity at ω and $\omega_{I,I'}$ is the molecular transition frequency between the vibronic levels I and I' of the ground electronic state. The Raman polarizability tensor elements are represented by $\alpha_{\sigma\rho}$, where the subscripts σ and ρ represent the three directions (x, y, z) in Euclidean space. In the resonance Raman (RR) scattering process, three different mechanisms are reported to be responsible for the selective enhancement of the Raman bands. According to Albrecht,[41] Raman tensor elements can be represented by three terms under RR conditions as follows:

$$\alpha_{\sigma\rho} = A + B + C \quad (4)$$

dx.doi.org/10.1021/jp204297y |J. Phys. Chem. C 2011, 115, 14309–14324

Table 3. Apparent Enhancement Factors (AEF) and Probable Tensor Elements (PTE) of Some Selected Raman Bands of the Molecule

A. AEF and PTE at Varied Adsorbate Concentrations

NRS solution (cm^{-1})	SERS (cm^{-1})	PTE (Sym)	AEF at various adsorbate concentrations			
			10^{-2} M	10^{-3} M	10^{-4} M	10^{-5} M
625	611	$\alpha_{xx};\alpha_{yy}$ (A′)	4.61×10^2	4.75×10^2	1.55×10^3	1.52×10^4
748	771	$\alpha_{yz};\alpha_{xz}$ (A″)	3.2×10^2	1.56×10^3	4.35×10^4	4.29×10^5
1326	1309	$\alpha_{xx};\alpha_{yy}$ (A′)	4.23×10^2	3.15×10^2	5.77×10^2	1.02×10^4
1362	1388	$\alpha_{xx};\alpha_{yy}$ (A′)	1.29×10^3	1.63×10^3	2.34×10^3	2.84×10^4
1521	1508	$\alpha_{xx};\alpha_{yy}$ (A′)	1.07×10^3	1.55×10^3	2.122×10^3	2.74×10^4
1656	1649	$\alpha_{xx};\alpha_{yy}$ (A′)	1.18×10^3	1.322×10^3	1.63×10^3	2.01×10^4

B. AEF at Varied pH Values for 1.0×10^{-2} Concentration

NRS solution (cm^{-1})	SERS (cm^{-1})	AEF at various pH		
		pH 2	pH 4	pH 7
625	611	6.92×10^2	2.95×10^2	4.61×10^2
1326	1309	2.75×10^2	1.56×10^2	4.23×10^2
1362	1388	1.19×10^3	6.59×10^2	1.29×10^3
1521	1508	1.1×10^3	8.86×10^2	1.07×10^3
1656	1649	9.86×10^2	8.26×10^2	1.18×10^3

The *A* term denotes a Franck−Condon (FC) contribution, while the *B* and *C* terms collectively represent Herzberg−Teller (HT) contributions. Lombardi et al.[42] recently suggested a unified theory concerning the enhancement mechanism of the SERS effect. A CT model for SERS, based on the theory of Albrecht has been proposed.[43] As in RR, the Raman polarizability tensor elements in SERS are also represented by the Albrecht's *A*, *B*, and *C* terms. Term *A* represents the FC contribution, and only totally symmetric vibrational modes are expected to be enhanced by this mechanism, as in the case of RR. The terms *B* and *C* in SERS arise from the HT contribution and are considered responsible for the selective enhancement of the Raman bands via molecule to metal CT and metal to molecule CT, respectively.[43,44] Both totally and nontotally symmetric vibrational modes may be enhanced by the *B* and *C* terms[43,44]

The metal to molecule CT interaction to SERS in the 3-TCA^- molecule may primarily be envisioned by considering the substantial red shift of the SERS bands centered at ∼611, 1308, 1362, and 1508 cm^{-1} with respect to their NRS counterparts as discussed in the preceding section. The appearance of the Ag−S and Ag−O vibrations at ∼155 and 225 cm^{-1} in the SERS spectra of the molecule may also portend considerable involvement of the CT mechanism to the overall SERS enhancement of the molecule.

The term *A* in the case of metal to molecule CT from a filled Fermi level *F* of the metal nanocolloid to the excited molecular state *K* is represented by[42,43]

$$A = (2/\hbar)\mu_{FK}^{\sigma}\mu_{FK}^{\rho}\langle i|k\rangle\langle k|f\rangle\frac{\omega_{FK} + \omega_f}{(\omega_{FK} + \omega_f)^2 - \omega^2} \quad (5)$$

where μ_{FK}^{σ} and μ_{FK}^{ρ} represent the electronic transition dipole moments from the Fermi level *F* of the metal to the affinity level of the excited molecular state *K* along the directions σ and ρ, respectively. The transition is possible because of the intensity borrowing via μ_{FK} through the allowed molecular transition from the ground vibronic state *I* to the excited vibronic state *K* of the molecule. In the above expression, ω signifies the frequency of the exciting laser radiation, while ω_f and ω_{FK} represent the frequency of vibration of the Fermi level of the metal and the transition frequency between the Fermi level *F* of the metal and the excited state *K* of the molecule, respectively.

The vibronic states *I*, *K*, and *F* are represented as the products of the electronic and vibrational wave functions:

$$|I\rangle = |I_e\rangle|i\rangle, \quad |K\rangle = |K_e\rangle|k\rangle, \quad |F\rangle = |F_e\rangle|f\rangle \quad (6)$$

The subscript *e* in the above expressions signifies a purely electronic state, and $|i\rangle$, $|k\rangle$, and $|f\rangle$ represent vibrational wave functions.

Equation 5, representing Albrecht's *A* term for SERS (under nonresonant conditions, as in the present case, which is away from molecular and surface plasmon resonances), becomes nonvanishing if the dipole transition moments μ_{FK}^{σ} and μ_{FK}^{ρ} and the vibrational overlap integral (FC factors) $\langle i|k\rangle\langle k|f\rangle$ are concurrently nonzero. For the FC factors to become nonzero, the basic requirement is the fulfillment of at least one of the following two conditions:

(i) There must exist a displacement of the minima in the potential energy surfaces (PES) of the two states involved in the transition ($\Delta Q_K \neq 0$) along a given normal coordinate *Q*.

(ii) There must be a change in the curvature of the PES ($\Delta\nu_K \neq 0$).

The CT mechanism in SERS may be considered to be analogous to a RR process; however, in SERS-CT, the transient exited state is a CT level of the metal−adsorbate (M−A) complex. The laser photon is thought to produce the resonant transfer of one electron from the metal to the vacant orbital of the adsorbate in the excited CT state (M^+-A^-). When the electron comes back to the metal, the electron−hole recombination generates a Raman photon, but the molecule remains

vibrationally excited. Thus, from the exclusive point of view of the adsorbed molecule, the resonant process takes place between the ground state of the anionic form (3-TCA$^-$) of the molecule (singlet S_0 electronic ground state of the adsorbate) and its dianion (doublet D_0 electronic ground state of the adsorbate). Detailed analyses of the above-mentioned model of the CT-SERS mechanism have been reported elsewhere.[45] The model has been considered to contemplate the metal to molecule CT-SERS process, as the case expected to be applicable in the SERS of the presently discussed probe molecule.

The displacement between the PES minima of the S_0 and the D_0 states are expressed as a function of normal coordinates (Q) of the ground state by the following relation:

$$\Delta Q = L^{-1}\Delta R \tag{7}$$

where L^{-1} is the inverse of the normal mode matrix of the S_0 state and ΔR is a vector that contains the differences between the optimized geometries of the states involved in the D_0-S_0 transitions. The ΔQ values thus obtained can be used to calculate the relative intensity of a Raman line under resonance conditions related to Albrecht's A term by using the Peticolas equation.[46]

$$I_i = K\Delta Q_i^2 \nu_i^3 \tag{8}$$

where K is constant and ν_i is the vibrational frequency of the i^{th} normal mode in the S_0 state.

The ΔQ values corresponding to the D_0-S_0 transition, calculated for the totally symmetric normal modes (A′) centered at ~611, 1308, 1362, 1508, and 1650 cm^{-1}, are 0.500276, −0.042501, −0.145745, 0.313038, and 0.068072 amu$^{1/2}$ Å, respectively. Thus, except for the bands centered at ~1308 and 1650 cm^{-1}, the ΔQ values for the other vibrational modes belonging to the A′ symmetry species of the molecule are quite appreciable. The genesis of the enhancement of the 611, 1362, and 1508 cm^{-1} bands in the SERS spectra of the molecule may primarily be due to the contribution from Albrecht's A term. Under resonant SERS-CT conditions, the selective enhancement of the above-mentioned SERS bands (at 611, 1362, and 1508 cm^{-1}) may indicate the presence of the forces acting on the molecule in the excited state. These forces depend on the difference between the equilibrium geometries of the adsobate (here 3-TCA$^-$) and their respective anion (here dianion; 3-TCA^{2-}), which are then analyzed through the ΔQ vector.[47] They are closely related to the shape of the virtual orbital, the LUMO of the adsorbate, shown in Figure 11, where the transferred electron is temporarily located. From Figure 11, it is clearly seen that the LUMO is mainly located on the thiazole ring moiety of the molecule, which may result in the shortening or enlargement of the bond lengths between the atoms, depending upon bonding or antibonding interactions of the respective π-orbitals. The resulting geometrical distortions of the thiazole ring moiety of the molecule closely resemble the Cartesian displacements of atoms associated with the vibrational modes at 611, 1362, and 1508 cm^{-1} shown in Figure 11. These results thus connote the predominant contribution of Albrecht's A term in the SERS-CT enhancement of the above-mentioned Raman bands.

The theoretically estimated relative SERS-CT intensities of the molecule using the Peticolas equation (eq 8) are 16, 1.2, 100, 12, and 15 for the 611, 1308, 1362, 1508, and 1650 cm^{-1} modes, respectively. The intensity profile is shown in Figure 12. The experimentally observed normalized intensity ratios (normalized

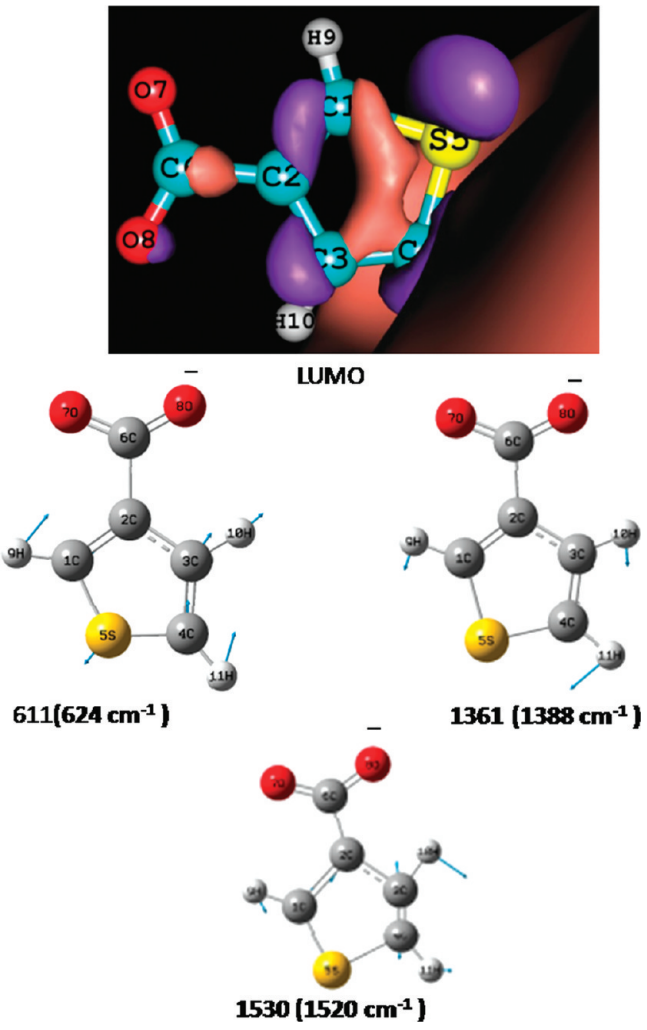

Figure 11. Shape of the LUMO obital of the 3-TCA$^-$ molecule (upper panel). Cartesian displacement and calculated (B3LYP/aug-cc-PVTZ) vibrational modes of the 3-TCA$^-$ molecule. Each number in parentheses refers to the experimental value of the assigned band (lower panel).

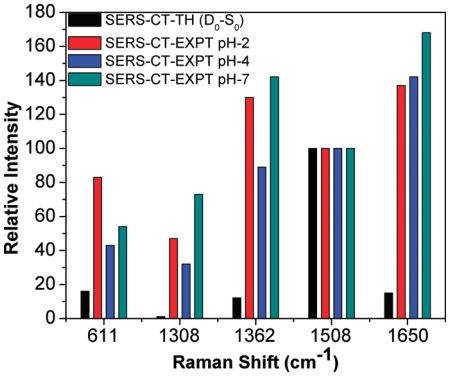

Figure 12. Intensity profile of theoretically simulated SERS-CT bands and experimentally observed SERS spectra of the molecule at 1.0×10^{-2} M adsorbate concentration for various pH values of the nanocolloidal silver surface.

for the 1508 cm^{-1} SERS band) of the above-mentioned SERS bands of the molecule at $C_{Ad} = 1.0 \times 10^{-2}$ M for various pH

dx.doi.org/10.1021/jp204297y |J. Phys. Chem. C 2011, 115, 14309–14324

values of the nanocolloidal silver surface are also shown in Figure 12. The intensity profile of the theoretically estimated SERS-CT bands and that of the experimentally observed SERS spectra are not in harmony, indicating the involvement of the EM contribution to SERS in addition to the CT effect for the above-mentioned vibrational signatures of the molecule. The moderate enhancement of the 1308 and 1650 cm^{-1} SERS bands belonging to the A′ symmetry species in the SERS spectra of the molecule may be ascribed somewhat weakly to moderate involvement of CT interaction via Albrecht's *A* term (considering the low but finite ΔQ values of the normal modes corresponding to the $D_0 - S_0$ transition), and the rest may be ascribed as from the EM contribution.

Interestingly, the band centered at ∼771 cm^{-1}, belonging to the A″ irreducible representation, is also enhanced significantly in the SERS spectra of the molecule. The enhancement of the A″ (nontotally symmetric) mode in the SERS spectra may not be accounted for from Albrecht's *A* term contribution and primarily connotes the CT effect of SERS through intensity borrowing from some allowed molecular transitions (the HT contribution) of the molecule.[42,43] The direction of CT in the case of the 3-TCA^- molecule adsorbed on a silver nanocolloid is from metal to molecule; hence, Albrecht's *C* term alone represents the HT contribution[42−44]

Albrecht's *C* term, according to the model of Lombardi et al.,[44] applicable for the SERS-CT effect, is represented as follows:

$$C = -(2/\hbar)\sum_{K\neq I}\frac{[\mu^{\sigma}_{KI}\mu^{\rho}_{FK} + \mu^{\rho}_{KI}\mu^{\sigma}_{FK}](\omega_{KI}\omega_{FK} + \omega^2)h_{IF}\langle i|Q|f\rangle}{(\omega^2_{KI} - \omega^2)(\omega^2_{FK} - \omega^2)} \quad (9)$$

where *i* and *f* are the initial and final quanta of the normal mode *Q*. μ_{FK} represents the electronic transitions from the Fermi level *F* of the metal to the affinity level of the excited state *K* of the molecule, which obtains its intensity through intensity borrowing from the allowed molecular transition $I \rightarrow K$. Here *I* represents the ground vibronic state of the molecule. Here μ_{IK} denotes the allowed molecular transition from the ground vibronic state *I* to the excited vibronic state *K*. The transition frequencies between $F \rightarrow K$ and $I \rightarrow K$ are represented by ω_{FK} and ω_{KI}, respectively, and ω signifies the incident laser frequency. The term h_{IF} in the above expression represents the vibronic coupling of the metal with the ground state of the molecule through some vibrational mode, called the HT coupling constant.

For the *C* term to be nonvanishing, the terms $\langle i|Q|f\rangle$, h_{IF}, μ_{KI}, and μ_{FK} must be simultaneously nonzero, and this fundamental prerequisite leads to the HT surface selection rule. The simplified expression of the HT surface selection rule is expressed as follows:[43,48]

$$\Gamma(Q_K) = \sum_K \Gamma(\mu^{\perp}_{CT})\Gamma_K \quad (10)$$

where $\Gamma(Q_K)$ is the irreducible representation belonging to the SERS active vibrational signature. $\Gamma(\mu^{\perp}_{CT})$ is the irreducible representation to which the component of the CT dipole moment perpendicular to the surface belongs in the combined molecule−metal system, and Γ_K is the irreducible representation of the molecular excited state to which the optical transition $(I \rightarrow K)$ is allowed. It is to be noted that the summation runs over all the allowed but presumably low-lying optical transitions.

Figure 13 shows the absorption spectrum of the probe molecule recorded in various solvent media (ca. methanol, acetonitrile, and cyclohexane) at neutral pH. The spectrum, as shown in Figure 13 is characterized by intense maxima at ∼203 and 237 nm, and both the peaks undergo small red shifts with a decrease in polarity of the solvent. This result may signify that the peaks of the absorption maxima at ∼203 and 237 nm are of $\pi \rightarrow \pi^*$ type, corresponding to $^1A'' \leftarrow {}^1A'$ and $^1A_{ex}' \leftarrow {}^1A'$ transitions. $^1A_{ex}'$ is the singlet excited state orbital symmetry. Table 4 shows the experimentally observed and theoretically predicted allowed transitions along with the oscillator strengths between the low-lying electronic states of the molecule. The HT selection rules may now be invoked (eq 10), and for the tilted or nearly flat orientation of the molecule, the CT dipole moment operator $(\mu^{\perp}_{CT})$ may be considered to be perpendicular to both the nanocolloidal surface and the molecular plane, so that $\Gamma(\mu^{\perp}_{CT}) = A''$. Thus, the CT states, according to HT selection rules, must be of A″ (A″ × A′) and A′ (A″ × A″) symmetries, corresponding to the UV transitions at 203 nm (calcd at 204.30 nm, f = 0.0026, $^1A'' \leftarrow {}^1A'$) and 237 nm (calcd at 224.97 nm, f = 0.1240, $^1A_{ex}' \leftarrow {}^1A'$), respectively. The HT intensity borrowing from the strongly allowed $^1A'' \leftarrow {}^1A'$ $(\pi \rightarrow \pi^*)$ and $^1A_{ex}' \leftarrow {}^1A'$ $(\pi \rightarrow \pi^*)$ transitions, in turn, allows the normal modes of vibration belonging to the irreducible representations A′ and A″ in the SERS spectra to be enhanced significantly via the contribution from Albrecht's *C* term. Thus, the enhancement of the SERS band at ∼771 cm^{-1} belonging to A″ irreducible representations may exclusively be accounted for from the CT contribution via the Albrecht's *C* term. However, the enhancements of the 1308 and 1650 cm^{-1} modes belonging to the A′ symmetry species in the SERS spectra of the molecule may be due to the following

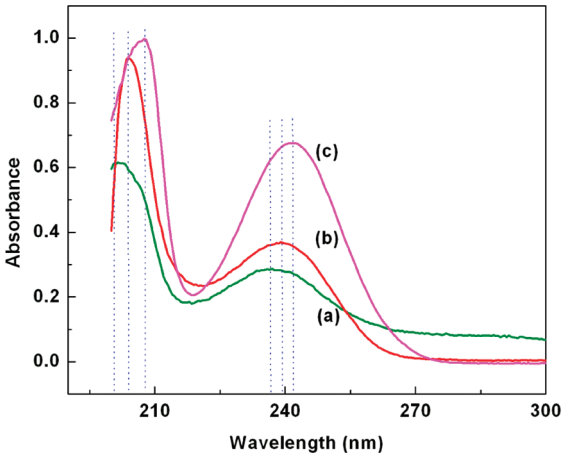

Figure 13. Room temperature UV−vis absorption spectra of the molecule at 4.0×10^{-3} M concentration in (a) acetonitile, (b) ethanol, and (c) cyclohexane solvent.

Table 4. Experimental and Theoretical Absorption Maxima of the Molecule

	λ_{max} (nm)			
transition	expt	calcd	oscillator strength (*f*)	symmetry (C_s)
$\pi \rightarrow \pi^*$	237	224	0.1240	$^1A'$
		222	0.0042	$^1A''$
		209	0.0001	$^1A''$
$\pi \rightarrow \pi^*$	203	204	0.0026	$^1A''$

reasons. (a) Considerable involvement of the Albrecht's *C* term, (b) weak involvement of the CT interaction via Albrecht's *A* term (considering low but finite ΔQ values of the normal modes corresponding to the D_0-S_0 transition), and (c) the rest from the EM contribution due to the coupling of the localized surface plasmons.

Thus, the above analyses allow us to understand the genesis of the enhancements of the 611, 1308, 1362, 1508, 1650, and 771 cm^{-1} SERS bands belonging to the A′ and A″ symmetry species respectively due to the CT contribution to SERS. Albrecht's *A* term plays a dominant role in the enhancement of the 611, 1362, and 1508 cm^{-1} bands, while, for the enhancement of the 771 cm^{-1} SERS band, Albrecht's *C* (i.e., the HT contribution) term plays a key role. However, both Albrecht's *A* and *C* terms may be responsible for the enhancement of the 1308 and 1650 cm^{-1} modes in the SERS spectra of the molecule.

5. CONCLUSION

The adsorption behavior of the industrially and biologically significant 3-thiophene carboxylic acid (3-TCA) molecules on the nanocolloidal silver surface has been investigated by SERS, aided by density functional theory. The optimized structural parameters of neutral and anionic forms of the molecule have been estimated from the above-mentioned level of theory. The vibrational modes of the molecule have been assigned. The concomitance of the Raman bands representing vibrational signatures emanating from the neutral and the anonic forms of the molecule signifies the presence of both the forms of the molecule in the solid state and in acetonitrile (ACN) solution. However, detailed vibrational analysis reveals that 54% of the neutral forms (3-TCA) of the molecule are prevalent in the solid state while 63% of the anionic forms (3-TCA^-) of the molecule predominate in ACN solution at neutral pH. SERS spectra recorded at various concentrations of the adsorbate and at various pH values both reveal that the anionic form of the molecule is adsorbed on the nanocolloidal silver surface with the molecular plane tilted or nearly flat with respect to the surface. The genesis of selective enhancements of the Raman bands at ∼611, 1308, 1362, 1508, 1650, and 771 cm^{-1} in the SERS spectra of the molecule has been unveiled from the view of Albretcht's *A* contribution and the Herzberg−Teller (HT) CT contribution. The Albrecht *A* term plays a dominant role in the enhancement of the 611, 1362, and 1508 cm^{-1} bands, while, for the enhancement of the 771 cm^{-1} SERS band, Albrecht's *C* (the HT contribution) term plays a key role. However, both Albrecht's *A* and *C* terms may be responsible for the enhancement of the 1308 and 1650 cm^{-1} modes in the SERS spectra of the molecule.

AUTHOR INFORMATION

Corresponding Author

*J.C.: tele fax, +91-33-2462-6869; e-mail, joydeep72_c@rediffmail.com. G.B.T.: telephone, +91-33-24734971; fax, +91-33-24732805; e-mail, spgbt@iacs.res.in.

Present Addresses

⊥Indian Association for the Cultivation of Science.

∥Department of Physics, Victoria Institution (College), 78 B, A. P. C. Road, Kolkata-700009, India.

#Department of Physics, Sammilani Mahavidyalaya, Baghajatin Station, E.M. Bypass, Kolkata-700075, India.

ACKNOWLEDGMENT

We thank DST, Government of India (Project No. SR/S2/CMP-0051/2006), for partial financial support. J.C. would like to thank the UGC, Government of India, for financial support through a research project (Project No. F. PSW-046/08-09 (ERO)). S.C. and J.C. are grateful to the authorities of IACS for providing the facilities needed to carry out the research work.

REFERENCES

(1) (a) Cortes, E.; Etchegoin, P. G.; Le Ru, E. C.; Fainstein, A.; Vela, M. E.; Salvarezza, R. C. *J. Am. Chem Soc.* **2010**, *132*, 18034. (b) Lombardi, J. R.; Birke, R. L.; Haran, G. *J. Phys. Chem. C* **2011**, *115*, 4540. (c) Kneipp, K.; Wang, Y.; Kneipp, H.; Perelman, L. T.; Itzkan, I.; Dasari, R. R.; Feld, M. S. *Phys. Rev. Lett.* **1997**, *78*, 1667. (d) Nie, S.; Emory, S. R. *Science* **1997**, *275*, 1102. (e) Pieczonka, N. P. W.; Aroca, R. F. *Chem. Soc. Rev.* **2008**, *37*, 946.

(2) (a) Lim, J. K.; Kwon, O.; Joo, S.-W. *J. Phys. Chem.* **2008**, *112*, 6816. (b) Pande, S.; Jana, S.; Sinha, A. K.; Sarkar, S.; Basu, M.; Pradhan, M.; Pal, A.; Chowdhury, J.; Pal, T. *J. Phys. Chem. C* **2009**, *113*, 6989. (c) Sarkar, S.; Pande, S.; Jana, S.; Sinha, A. K.; Pradhan, M.; Basu, M.; Chowdhury, J.; Pal, T. *J. Phys. Chem. C* **2008**, *112*, 17862. (d) Aliaga, A. E.; Garrido, C.; Leyton, P. G.; Diaz, F.; Gomez-Jeria, J. S.; Aguayo; Clavijo, T.; Campos-Vallette, E. M.; Sanchez-Cortes, M. S. *Spectrochim. Acta, Part A* **2010**, *76*, 458. (e) Ansar, S. M.; Haputhanthri, R.; Edmonds, B.; Liu, D.; Yu, L.; Sygula, A.; Zhang, D. *J. Phys. Chem. C* **2010**, *115*, 653.

(3) Chowdhury, J.; Sarkar, J.; Tanaka, T.; Talapatra, G. B. *J. Phys. Chem. C* **2008**, *112*, 227–239.

(4) (a) Costa, J. C. S.; Ando, R. A.; Camargo, P. H. C.; Corio, P. *J. Phys. Chem. C* **2011**, *115*, 4184. (b) Sarkar, J.; Chowdhury, J.; Ghosh, M.; De, R.; Talapatra, G. B. *J. Phys. Chem. B* **2005**, *109*, 12861–12867. (c) Sarkar, J.; Chowdhury, J.; Ghosh, M.; De, R.; Talapatra, G. B. *J. Phys. Chem. B* **2005**, *109*, 22536–22544.

(5) (a) Sanchez-Gil, J. A.; Garcia-Ramos, J. V. *Chem. Phys. Lett.* **2003**, *367*, 361. (b) Garcia-Vidal, F. J.; Pendry, J. B. *Phys. Rev. Lett.* **1996**, *77*, 1163. (c) Sanchez-Gil, J. A.; Garcia-Ramos, J. V.; Mendez, E. R. *Phys. Rev. B* **2001**, *62*, 10515. (d) Sanchez-Gil, A. J.; Garcia-Ramos, V.; Mendez, E. R. *Phys. Rev. B* **2001**, *62*, 10515. (e) Rojas, V. R.; Claro, F. *J. Chem. Phys.* **1993**, *98*, 998. (f) Zhao, L.; Jensen, L.; Schatz, G. C. *J. Am. Chem. Soc.* **2006**, *128*, 2911.

(6) (a) Moskovits, M. *Rev. Mod. Phys.* **1985**, *57*, 783. (b) Kneipp, K.; Kneipp, H.; Itzkan, I.; Dasari, R. R.; Feld, M. S. *Chem. Rev.* **1999**, *99*, 2957. (c) Sackmann, M.; Materny, A. *J. Raman Spectrosc.* **2006**, *37*, 305. (d) Campion, A.; Kambhampati, P. *Chem. Soc. Rev.* **1998**, *27*, 241. (e) Schatz, G. C.; Young, M. A.; Van Duyne. In *Surface-Enhanced Raman Scattering: Physics and Applications*; Kneipp, K., Moskovits, M., Kneipp, H., Eds.; Topics in Applied Physics; Springer: Berlin, New York, 2006; Vol. 103. (f) Jensen, L.; Aikens, C. M.; Schatz, G. C. *Chem. Soc. Rev.* **2008**, *37*, 1061. (g) Kneipp, J.; Kneipp, H.; Kneipp, K. *Chem. Soc. Rev.* **2008**, *37*, 1052.

(7) (a) Camden, J. P.; Dieringer, J. R.; Zhao, J.; Van Duyne, R. P. *Acc. Chem. Res.* **2008**, *41*, 1653. (b) Le Ru, E. C.; Etchegoin, P. G. *J. Chem. Phys.* **2009**, *130*, 181101. (c) Kelley, A. M. *J. Chem. Phys.* **2008**, *128*, 224702. (d) Vernon, K. C.; Davis, T. J.; Scholes, F. H.; Gomez, D. E.; Lau, D. *J. Raman Spectrosc.* **2010**, *41*, 1106.

(8) (a) Lombardi, J. R.; Birke, R. L; Lu, T.; Xu, J. *J. Chem. Phys.* **1986**, *84*, 4174. (b) Arenas, J. F.; Woolley, M. S.; López Tocón, I.; Otero, J. C.; Marcos, J. I. *J. Chem. Phys.* **2000**, *112*, 7669. (c) Dieringer, J. A.; McFarland, A. D.; Shah, N. C.; Stuart, D. A.; Whitney, A. V.; Yonzon, C. R.; Young, M. A.; Zhang, X.; Van Duyne, R. P. *Faraday Discuss.* **2006**, *132*, 9. (d) Lombardi, J. R.; Birke, R. L. *J. Phys. Chem. C* **2008**, *112* (5605), 24. (e) Lopez-Ramirez, M. R.; Ruano, C.; Castro, J. L.; Arenas, J. F.; Soto, J.; Otero, J. C. *J. Phys. Chem. C* **2010**, *114*, 7666. (f) Morton, S. M.; Jensen, L. *J. Am. Chem. Soc.* **2009**, *131*, 4090. (g) Liu, S.; Li, X. Y.; Zhao, X.; Chen, M. *J. Chem. Phys.* **2009**, *130*, 234509. (h) Fu, X.; Pan, Y.; Wang, X.; Lombardi, J. R. *J. Chem. Phys.* **2011**, *134*, 024707. (i) Wu

D.-Y.; Hayashi, M.; Chang, C. H.; Liang, K. K.; Lin, S. H. *J. Chem. Phys.* **2003**, *118*, 4073.

(9) (a) Papadopoulou, E.; Bell, S. E. J. *J. Phys. Chem.* **2010**, *114*, 22644. (b) Brewer, K. E.; Aikens, C. M. *J. Phys. Chem A* **2010**, *114*, 8858. (c) Wu, D.-Y.; Liu, X.-M.; Huang, Y.-F.; Ren, B.; Xu, X.; Tian, Z. Q. *J. Phys. Chem. C* **2009**, *113*, 18212. (d) Muniz-Miranda, M.; Gellini, C.; Pagliai, M.; Innocenti, M.; Salvi, P. R.; Schettino, V. *J. Phys. Chem. C* **2010**, *114*, 13730. (e) Biswas, N.; Thomas, S.; Sarkar, A.; Mukherjee, T.; Kapoor, S. *J. Phys. Chem. C* **2009**, *113*, 709. (f) Aliaga, A. E.; Ahumada, H.; Sepulveda, K.; Gomez-Jeria, J. S.; Garrido, C.; Weiss-Lopez, B. E.; Campos-Vallette, M. M. *J. Phys. Chem. C* **2011**, *115*, 3982–3989. (g) Wu, D. Y.; Hayashi, M.; Lin, S. H.; Tian, Z. Q. *Spectrochim. Acta A* **2004**, *60*, 137. (h) Pagliai, M.; Muniz-Miranda, M.; Cardini, G.; Schettino, V. *J. Phys. Chem. A* **2009**, *13*, 15198.

(10) Katrizky, A. R., Rees, C. W., Scriven, E. F. V., Eds. *Comprehensive Heterocyclic Chemistry II*; Pergamon Press: Oxford, 1996; Vol. 2.

(11) Phillion, D. P.; Braccolino, D. S.; Graneto, M. J.; Phillips,W. G.; Van Sant, K. A.; Walker, D. M.; Wong, S. C. European Patent CODEN: EPXXDW1992, 1993, *711*, EP 538231 A 1 19930421.

(12) Samarkandy, A. A.; Al- Youbi, A. O.; Khalil, R. M.; Fattah, A. A. A. *Bull. Electrochem.* **2001**, *17*, 111.

(13) Chi-te, C.; Kuo-mou, C.; Wann- huang, L.; Fen-lan, L.; Rong-tsun, W. U.S. Patents 5602170 (1997), 5747525 (1998), 5753692 (1998).

(14) Minkin, C. V. S; Goldhaber, P. *Science* **1971**, *172*, 163.

(15) (a) Roncali, J. *Chem. Rev.* **1992**, *92*, 711. (b) Mecullough, R. D. *Adv. Mater.* **1998**, *10*, 93. (c) Kline, R. J.; McGhee, M. D.; Toney, M. F. *Nat. Mater.* **2006**, *5*, 197. (d) McQuade, D. T.; Pullen, A. E.; Swagar, T. M. *Chem. Rev.* **2000**, *100*, 2537.

(16) (a) Temprado, M.; Roux, M. V.; Jimenez, P.; Davalos, J. Z.; Notario, R. *J. Phys. Chem. A* **2002**, *106*, 11173. (b) Roux, M. V.; Temprado, M.; Jimenez, P.; Davalos, J. Z.; Foces, C. F.; Garcia, M. V.; Redondo, M. I. *Thermochim. Acta* **2003**, *404*, 235.

(17) Creighton, J. A.; Blatchford, C. G.; Albrecht, M. G. *J. Chem. Soc., Faraday Trans.* **1979**, *275*, 790.

(18) Chowdhury, J.; Ghosh, M.; Misra, T. N. J. *Colloid Interface Sci.* **2000**, *228*, 372.

(19) Frisch, M. J.; Trucks, G. W.; Schiegel, H. B.; Scuseria, G. E.; Robb, M. A.; Cheeseman, J. R.; Montgomery, J. A.; Vreven, T., Jr.; Kudin, K. N.; Burant, J. C.; Millam, J. M.; Iyengar, S. S.; Tomasi, J.; Barone, V.; Mennucci, B.; Cossi, M.; Scalmani, G.; Rega, N.; Petersson, G. A.; Nakatsuji, H.; Hada, M.; Ehara, M.; Toyota, K.; Fukuda, R.; Hasegawa, J.; Ishida, M.; Nakajima, T.; Honda, Y.; Kitao, O.; Nakai, H.; Klene, M.; Li, X.; Knox, J. E.; Hratchian, H. P.; Cross, J. B.; Adamo, C.; Jaramillo, J.; Gomperts, R.; Stratmann, R. E.; Yazyev, O.; Austin, A. J.; Cammi, R.; Pomelli, C.; Ochterski, J. W.; Ayala, P. Y.; Morokuma, K.; Voth, G. A.; Salvador, P. J.; Dannenberg, J.; Zakrzewski, V. G.; Dapprich, S.; Daniels, A. D.; Strain, M. C.; Farkas, O.; Malick, D. K.; Rabuck, A. D.; Rahgavachari, K.; Foresman, J. B.; Ortiz, J. V.; Cui, Q.; Baboul, A. G.; Clifford, S.; Cioslowski, J.; Stefanov, B. B.; Liu, G.; Liashenko, A.; Piskorz, P.; Komaromi, I.; Martin, R. L.; Fox, D. J.; Keith, T.; Al-Laham, M. A.; Peng, C. Y.; Nanayakkara, A.; Challacombe, M.; Gill, P. M. W.; Johnson, B.; Chen, W.; Wong, M. W.; Gonzalez, C.; Pople, J. A. *Gaussian 03*; Gaussian, Inc.: Pittsburgh, PA, 2003.

(20) Perdew, J. P.; Wang, Y. *Phys. Rev. B* **1992**, *45*, 13244.

(21) (a) Dunning, T. H., Jr. *J. Chem. Phys.* **1989**, *90*, 1007. (b) Woon, D. E.; Dunning, T. H., Jr. *J. Chem. Phys.* **1994**, *100*, 2975. (c) Dunning, T. H., Jr. *J. Chem. Phys.* **1989**, *90*, 1007. (d) Woon, D. E.; Dunning, T. H., Jr. *J. Chem. Phys.* **1993**, *98*, 1358.

(22) Martin, J. M. L.; Van Alsenoy, C. *GAR2PED*; University of Antwerp: 1995.

(23) Morita, S. 2Dshige; Kwansei-Gakuin University: 2004−2005.

(24) Marvin 5.1.0, ChemAxon (http://www.chemaxon.com), 2008.

(25) Bak, B.; Christensen, D.; Hansen-Nygaard, L.; Rastrup-Andersen, J. J. *Mol. Spectrosc.* **1961**, *7*, 58.

(26) (a) Aroca, R. F.; Clavijo, R. E.; Halls, M. D.; Schlegel, H. B. *J. Phys. Chem. A* **2000**, *104*, 9500. (b) Bolboaca, M.; Iliescu, T.; Paizs, Cs.; Irimie, F. D.; Kiefer, W. *J. Phys. Chem. A* **2003**, *107*, 1811.

(27) Sarkar, J.; Chowdhury, J.; Talapatra, G. B. *J. Phys. Chem. C* **2007**, *111*, 10049–10061.

(28) (a) Rico, M.; Orza, J. M. *J. Morcillo Spectrochim. Acta* **1965**, *21*, 689. (b) Samagne, J. J. P.; Lebas, J. B. *Spectrochim. Acta* **1970**, *26A*, 1651. (c) Piliani, G.; Cataliotti, R. *Spectrochim. Acta* **1982**, *38A*, 751. (d) Horak, M.; Hyams, I. J.; Hyams, E. R. *Spectrochim. Acta* **1966**, *22A*, 1355. (e) Piliani, G.; Cataliotti, R. *Spectrochim. Acta* **1981**, *37A*, 707. (f) Sarkar, U. K. *Chem. Phys. Lett.* **2003**, *374*, 341.

(29) Lapinski, L.; Nowak, M. J.; Kwaitkowski, J. S.; Leszczynski, J. *J. Phys. Chem. A* **1999**, *103*, 280.

(30) Chowdhury, J.; Ghosh, M. J. *Colloid Interface Sci.* **2004**, *277*, 121.

(31) Sanda, P. N.; Warlaumont, J. M.; Demuth, J. E.; Tsang, J. C.; Christmann, K.; Bradley, J. A. *Phys. Rev. Lett.* **1980**, *45*, 1519.

(32) (a) Bowmaker, G. A.; Tan, L. C. *Aust. J. Chem.* **1979**, *32*, 1443. (b) Loo, B. H. *Chem. Phys. Lett.* **1982**, *89*, 346. (c) Sanchez-Cortes, S.; Garcia-Ramos, J. V. *J. Raman Spectrosc.* **1992**, *23*, 61.

(33) (a) Zhang, D.; Ansar, S. M. *Anal. Chem.* **2010**, *82*, 5910. (b) Ansar, S. M.; Haputhanthri, R.; Edmonds, B.; Liu, D.; Yu, L.; Sygula, A.; Zhang, D. *J. Phys. Chem. C* **2011**, *115*, 653.

(34) (a) Mukherjee, K.; Bhattacharjee, D.; Misra, T. N. *J. Colloid Interface Sci.* **1997**, *193*, 286. (b) Mukherjee, K.; Bhattacharjee, D.; Misra, T. N. *J. Colloid Interface Sci.* **1999**, *213*, 46. (c) Mukherjee, K.; Misra, T. N. *Spectrochim. Acta* **1997**, *53 A*, 1439. (d) Mukherjee, K.; Misra, T. N. *Bull. Chem. Soc. Jpn.* **1997**, *70*, 301.

(35) (a) Chowdhury, J.; Mukerjee, K. M.; Misra, T. N. *J. Raman Spectrosc.* **2000**, *31*, 427. (b) Sanchez-Cortes, S.; Garcia-Ramos, J. V. *J. Raman Spectrosc.* **1990**, *21*, 679.

(36) (a) Bukowska, J. *J. Mol. Struct.* **1992**, *275*, 151. (b) Compagnini, G.; De Bonis, A.; Cataliotti, R. S.; Marletta, G. *Phys. Chem. Chem. Phys.* **2000**, *2*, 5298. (c) Bazzaoui, E. A.; Levi, G.; Aeiyach, S.; Aubard, J.; Marsault, J. P.; Lacaze, P. C. *J. Phys. Chem.* **1995**, *99*, 6628. (d) Kim, H.-J.; Kim, D.-C.; Kim, R.; Kim, J.; Park, D.-H.; Kim, H.-S.; Joo, J.; Suh, Y. D. *J. Appl. Phys.* **2007**, *101*, 053514. (e) Shen, Y.; Chen, F.; Wu, P.; Shi, G. *J. Chem. Phys.* **2003**, *119*, 11415. (f) Pathak, S.; Kumar, A.; Tandon, P.; Kiskan, B.; Koz, B.; Yagci, Y. E. *Polym. J.* **2010**, *46*, 1525. (g) Fujita, W.; Teramae, N.; Haraguchi, H. *Chem. Lett.* **1994**, *23*, 511. (h) Shi, G.; Xu, J.; Fu, M. *J. Phys. Chem. B* **2002**, *106*, 288. (i) Chen, F.; Shi, G.; Zhang, J.; Fu, M. *Thin Solid Films* **2003**, *424*, 283.

(37) (a) Noda, I.; Ozaki, Y. In *Two-Dimensional Correlation Spectroscopy, Applications in Vibrational and Optical Spectroscopy*; John Wiley and Sons: England, 2004. (b) Sett, P.; Chowdhury, J.; Mallick, P. K. *Chem. Phys. Phys. Lett.* **2008**, *464*, 87.

(38) Moskovits, M.; Suh, J. *J. Phys. Chem.* **1984**, *88*, 1293.

(39) Tourwe, Els; Baert, K.; Hubin, A. *Vib. Spectrosc.* **2006**, *40*, 25.

(40) Moskovits, M. *J. Chem. Phys.* **1982**, *77*, 4408. Creighton, J. A. *Surf. Sci.* **1983**, *124*, 209.

(41) Albrecht, A. C. *J. Chem. Phys.* **1961**, *34*, 1476.

(42) Lombardi, J. R.; Birke, R. L. *J. Phys. Chem. C* **2008**, *112*, 5605.

(43) Lombardi, J. R.; Birke, R. L.; Lu, T.; Xu, J. *J. Chem. Phys.* **1986**, *84*, 4174.

(44) Osawa, M.; Matsuda, N.; Yoshii, K.; Uchida, I. *J. Phys. Chem.* **1994**, *98*, 12702.

(45) (a) Arenas, J. F.; Woolley, M. K.; Lopez Tacon, I.; Otero, J. C.; Marcos, J. I. *J. Chem. Phys.* **2000**, *112*, 7669. (b) Arenas, J. F.; Soto, J.; Lopez Tacon, I.; Fernandez, D. J. J.; Otero, C.; Marcos, I. J. *J. Chem. Phys.* **2002**, *116*, 7207.

(46) Peticolas, W. L.; Strommen, D. P.; Lakshminarayanan, V. *J. Chem. Phys.* **1980**, *73*, 4185.

(47) (a) Lopez-Ramirez, M. R.; Ruano, C.; Castro, J. L.; Arenas, J. F.; Soto, J.; Otero, J. C. *J. Phys. Chem. C* **2010**, *114*, 7666. (b) Avila, F.; Soto, J.; Arenas, J. F.; Rodriguez, J. A.; Palaez, D.; J. Otero, C. *J. Phys. Chem. C* **2009**, *113*, 105.

(48) (a) Canamares, M. V.; Chenal, C.; Birke, R. L.; Lombardi, J. R. *J. Phys. Chem. C* **2008**, *112*, 20295. (b) Chenal, C.; Birke, R. L.; Lombardi, J. R. *Chem. Phys. Chem.* **2008**, *9*, 1617.